Assembling a supramolecular 3D network with tuneable mechanical properties using adamantylated cross-linking agents and β-cyclodextrin-modified hyaluronan

Assembling a supramolecular 3D network with tuneable mechanical properties using adamantylated cross-linking agents and P-cyclodextrin-modified hyaluronan

Marek Jurtíka,1, Barbora Gresková a,1 Zdeňka Pruckovaa, Michal Rouchala, Lenka Dastychová a, Lenka Vítková b, Kristýna Valaskovac, Eva Achbergerová d, Robert Víchaa,*

[a] *Department of Chemistry, Faculty of Technology, Tomas Bata University in Zlín, Vavreřkova 5669, 760 01 Zlín, Czech Republic*

[b] *Department of Physics and Materials Engineering, Faculty of Technology, Tomas Bata University in Zlín, Vavrečkova 5669, 760 01 Zlín, Czech Republic*

[c] *Centre of Polymer Systems, Tomas Bata University in Zlín, třída T. Bati 5678, 760 01 Zlín, Czech Republic*

[d] *CEBIA-Tech, Faculty of Applied Informatics, Tomas Bata University in Zlín, Nad Stranřmi 4511, 760 05 Zlín, Czech Republic*

** Corresponding author. E-mail address: rvicha@utb.cz (R. Vícha).*

ABSTRACT

Hydrogels based on the supramolecular host-guest concept can be prepared if at least one constituent is a polymer chain modified with supramolecular host or guest (or both) units. Low-molecular-weight multitopic counterparts can also be used, however, guest molecules in the role of cross-linking agents are seldom reported, although such an approach offers wide-ranging possibilities for tuning the system properties via easily achievable structural modifications. In this paper, a series of adamantane-based star-like guest molecules was used for crosslinking of two types of β-cyclodextrin-modified hyaluronan (CD-HA). The prepared 3D supramolecular networks were characterised using nuclear magnetic resonance, titration calorimetry and rheological measurements to confirm the formation of the host-guest complexes between adamantane moieties and β-cyclodextrin units, including their typical properties such as self-healing and dynamic nature. The results indicate that the nature of the cross-linker (amides versus esters) has a greater impact on mechanical properties than the length of the guest's arms. In addition, the results show that the length of the HA polymer chain is more important than the degree of modification with supramolecular units. In conclusion, it was proven that the modular concept employing low-molecular-weight cross-linking guests is valuable for the formulation of supramolecular networks, including hydrogels.

Keywords: Host-guest systems, 3D network, Physical cross-linking, Adamantane, Hyaluronic acid

1. Introduction

Hydrogels represent intriguing materials widely prepared and tested for applications in tissue engineering (Lei et al., 2022; Zhou et al., 2022a; Zhou et al., 2022b), drug delivery (Mealy et al., 2015; Phua et al., 2019; Rowland et al., 2018), bioimaging (Dai et al., 2022; Zhang et al., 2021), energy storage (Huang et al., 2022a; Yang et al., 2020), sensing (Gao et al., 2020; Huang et al., 2021; Mo et al., 2021) and environmental restoration (Alizadehgiashi et al., 2018; Tang et al., 2020). In addition to hydrogels

based on artificial poly(vinyl alcohol) (Wu et al., 2021; Yao et al., 2020; Zhang et al., 2012), poly(ethylene glycol) (Kolewe et al., 2018; Sinha et al., 2023) or poly(acrylate) (Liu et al., 2022a; Yuan et al., 2021), materials derived from natural biopolymers, e.g. alginates (Ghaderinejad et al., 2021; Zhang et al., 2022b; Zhu et al., 2022), cellulose (Hu et al., 2021b; Shu et al., 2022; Zhang et al., 2022a), chitosan (Burillo et al., 2021; Jin et al., 2021; Li et al., 2022b), heparin (Li et al., 2022a; Nilasaroya et al., 2021), fibrin (Jarrell et al., 2021; Sudhadevi et al., 2021; Ziemkiewicz et al., 2022) and hyaluronic acid (Chen et al., 2021; Li et al., 2022d; Zhang et al., 2022c) have become very attractive in past decades. However, these natural polymers display insufficient stability against biodegradation and non-enzymatic decomposition. Therefore, chemical modification of the original materials, which is frequently followed by cross-linking of the polymer chains, is employed to improve the hydrogel properties (Liu et al., 2022b; Mueller et al., 2022; Muir & Burdick, 2021).

In general, hydrogels can be prepared using three distinct types of cross-linking, i.e. covalent, dynamic covalent and physical. The most common approaches used for the preparation of covalently cross-linked hydrogels are free radical chain polymerisation (Kang et al., 2017), click chemistry (Engkagul et al., 2018; Ji et al., 2020) and oxidation of phenolic groups (Shin et al., 2020). Hydrogels based on dynamic covalent cross-linking can be formed, for example, using Schiff's base reactions (Boehnke et al., 2015; Wang et al., 2018; Xu et al., 2018; Xue et al., 2022), disulphide formation (Bermejo-Velasco et al., 2019), acyl hydrazone bonds (Hu et al., 2021a; Xue et al., 2022) or the Diels-Alder reaction (Bi et al., 2019). These two approaches are disadvantaged due to probable contamination of the final material with residual reagents, catalysts and/or undesired side products. Therefore, tests for biocompatibility are needed for each prepared batch of the material. Finally, non-covalent interactions, such as host-guest complexation (Xu et al., 2019; Zhang et al., 2020), hydrogen bonding (Hou et al., 2015; Mol et al., 2019) and metal-ligand coordination (Shin et al., 2019; Yavvari et al., 2017), were used for the preparation of physically cross-linked hydrogels within past two decades.

Hydrogels based on non-covalent interactions between their molecular constituents have some specific properties (Xia et al., 2020; Yang et al., 2022). Highly advantageous is that a supramolecular network is formed in situ by simple mechanical mixing of the components. These components are synthesised, purified, and tested for toxicity individually before the preparation of the final material. Therefore, contamination of the final hydrogel with any undesired chemical compounds is avoided. Since the host-guest pairs are formed in a thermodynamic equilibrium manner, the linking is reversible and such systems are inherently self-healing (Saunders & Ma, 2019). Finally, the properties of the hydrogel can be easily tuned and varied, either by structural modification of components or by the addition of competitors that can modulate the number of host-guest interactions involved in a supra-molecular network. On the other hand, there are certain inconveniencies related to the supramolecular nature. Molecular components are usually soluble in the environment used for gel preparation. Therefore, further stabilisation of the final material is needed, for instance, by the employment of additional orthogonal host-guest interactions (Chen et al., 2023).

Considering the host-guest supramolecular concept, there are several approaches in preparing a supramolecular network, however, all of them employ molecular components with multiple supramolecular units. The first approach uses two graft polymers: one modified with host moieties and the second bearing guest units (Rosales et al., 2018). For example, Neisi et al. published the preparation of fully biocompatible and low-cost supramolecular hydrogels based on cross-linking between cellulose nanowhiskers modified using gallic acid and β-cyclodextrin (β-CD), respectively (Neisi et al., 2023). Recently, a hybrid double network hydrogel potentially used as a carrier system for water-insoluble drugs was developed by Li et al. (2022c). In addition, linear or dendrimer-like polymers terminated with adamantane-based binding motifs were used as cross-linkers for hydrogel

preparations (Chen et al., 2018; Ooi et al., 2020; Yu et al., 2020). The polymeric nature and random modification of the polymer backbone bring serious difficulties for an exact description of the relations between the properties of the system and the structure of the components. To reduce this issue, one polymeric component can be replaced with low-molecular-weight chemical individuals, as discussed below. The second approach was enabled by the discovery of cucurbit[n]uril (CBns) hosts in the last two decades of the 20th century (Freeman et al., 1981; Kim et al., 2000), which provides the tightest host-guest complexes (Cao et al., 2014). Since the modified CBns are not easily available on a large scale, the polymer chain is decorated with a suitable guest, which forms a sandwich-like 2:1 complex with sufficiently large CBns homolog (typically methyl viologen, imidazolium or naphthalene derivatives with CB8) (Huang et al., 2020; Huang et al., 2022b; Wu et al., 2017). However, cucurbit[n]urils remain very expensive even forty years after their discovery. Thus, large-scale production of CBn-based materials is unavailable. Finally, the polymer modified with one supramolecular motif can be cross-linked with low-molecular-weight agents bearing multiple supramolecular counterparts. There are several examples in literature of guest-modified polymers, which are cross-linked with multitopic host agents (Lu et al., 2022; Wei et al., 2016). Surprisingly, the inverse approach, i.e. polymers decorated with host units and multitopic guests is only rarely reported (Gao et al., 2022; Kwon et al., 2015) despite its obvious advantage. From a synthetic perspective, structural modifications on low-molecular-weight multitopic guests are much easier to perform to reach a great portfolio of cross-linkers with variable properties.

The choice of adamantane derivatives and β-CD as the supramolec-ular guest-host pair can be justified by perfect geometrical compatibility, which enables high-affinity binding, and the synthetic availability of many various derivatives. An adamantane cage is a geometrically rigid, highly symmetric hydrocarbon structure that is excellently resistant to a wide range of redox and acidic/basic conditions. Its derivatives are easily available, many of them from commercial sources. Cyclo-dextrins are natural products of starch fermentation (Crini, 2014). The most common homologues, i.e. α-CD, β-CD and γ-CD consisting of six, seven and eight glucose units, respectively, are well-recognised as nontoxic and biocompatible supramolecular carriers and have been used in many biomedical applications (Trotta et al., 2022). Adamantane derivatives and β-CD, which has an interior cavity geometrically compatible with the adamantane cage, provide extraordinarily stable host-guest complexes within the cyclodextrin family. The association constants of 1:1 aggregates reach the order of 10^6 M^{-1} (Tomecek et al., 2021; Zatloukal et al., 2021). This means that there is a significant portion of complexed counterparts, even at concentrations of about 0.1 mM. Indeed, there are some hosts, namely cucurbit[7]uril, that provide much higher affinities towards adamantane-based guests (Barrow et al., 2015). Unfortunately, singly substituted derivatives of these macrocycles are not available for polymer modification in sufficient quantities. Finally, due to the lipophilic nature of the adamantane cage and interior cavity of CD, the hydrophobic effect is the most important force holding the components together. Thus, the Ad@β-CD complexes are the most stable in an aqueous environment and are not disrupted by H-bonding with other mixture components and/or solvent molecules.

To the best of our knowledge, no paper describing the preparation and rheologic properties of supramolecular networks consisting of adamantylated low-molecular-weight cross-linkers and cyclodextrin-modified biopolymer has been published so far. Presented herein is a case study on a set of adamantane-based, virtually C_{3h} symmetric, tritopic guests that were used for cross-linking of β-cyclodextrin-modified hyaluronan (CD-HA) to form 3D supramolecular networks. This study attempts to verify a hypothesis that multitopic low-molecular guests can act as modular cross-linking agents with the ability to tune the physical properties of the gel with simple structural modifications.

2. Results and discussion

2.1. Syntheses

The tritopic supramolecular cross-linkers were synthesised according to **Scheme 1**. Initially, adamanatane-1-carbonyl chloride was reacted with various ethylene glycol-like linkers to form either amides 5a, 5b or esters 5c-5e. Similarly, these adamantylated arms were linked via ester or amide bond to the central unit based on benzene-1,3,5-tricarboxylic acid (1b). In addition to NMR and IR (for spectra, see Supporting Information) the final tritopic guests were characterised using mass spectrometry. It was revealed that these compounds form relatively stable complexes with singly charged alkali metals (Li^+, Na^+, K^+ and Cs^+) and significantly weaker complexes with alkaline earth metals (Mg^{2+}, Ca^{2+} and Ba^{2+}). For more details, see Supporting Information, Fig. S23. Since the final compounds 6a-6e were sparingly soluble in the water, mixtures of water and acetonitrile (MeCN) were used for all further experiments on the supramolecular networks.

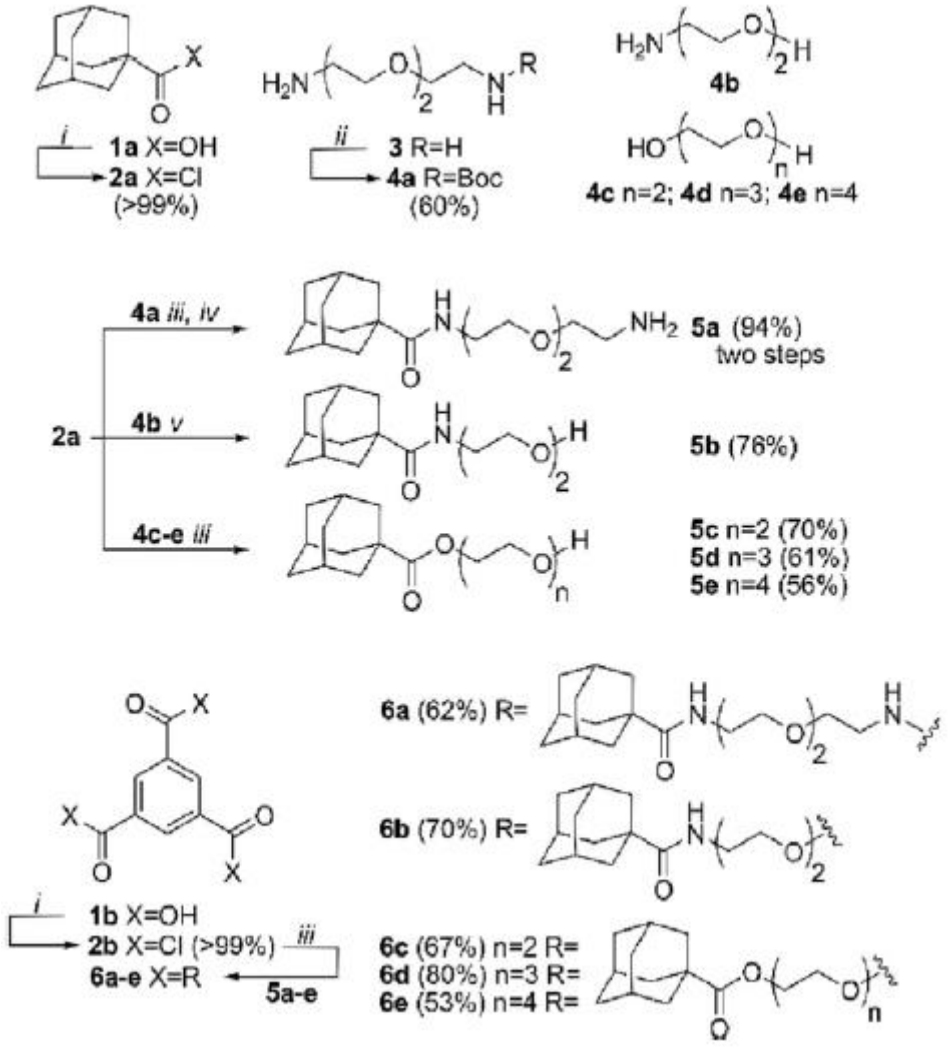

Scheme 1. Synthesis of tritopic supramolecular linkers. i $SOCl_2$, DMF (catalytic amount), reflux, 3 h; ii Boc_2O, DCM, 0 °C → rt, overnight; iii DCM, TEA, 0 °C → rt, overnight; iv TFA, DCM, rt; v DCM, 0 °C → rt, overnight.

The CD-HAs were prepared via a click reaction (1,3-dipolar cycloaddition) between azidocyclodextrin 9 and propargylated HA 11 or 13 (see Scheme 2). Monoazido-p-cyclodextrin 9 was prepared according to a previously published procedure, as shown in Scheme S1 in Supporting Information. Several difficulties were faced when purifying compound 9, since dialyses using a 500 MW cut-off column (Nielsen et al., 2010) led to an unacceptable loss of the material. The typical recovery of pure 9 was <40 % in 5 days. Indeed, dialysis within 3 days afforded up to 60 % of 9, however, this material was still contaminated with an inorganic azide. Therefore, cation/anion-exchange Amberlite MB-2 resin (Petter et al., 1990) was used to achieve excellent purity and essentially quantitative recovery of the cyclodextrin 9 within a 2-h operation. The content of inorganic azide was monitored using IR spectroscopy, as seen in Fig. S24.

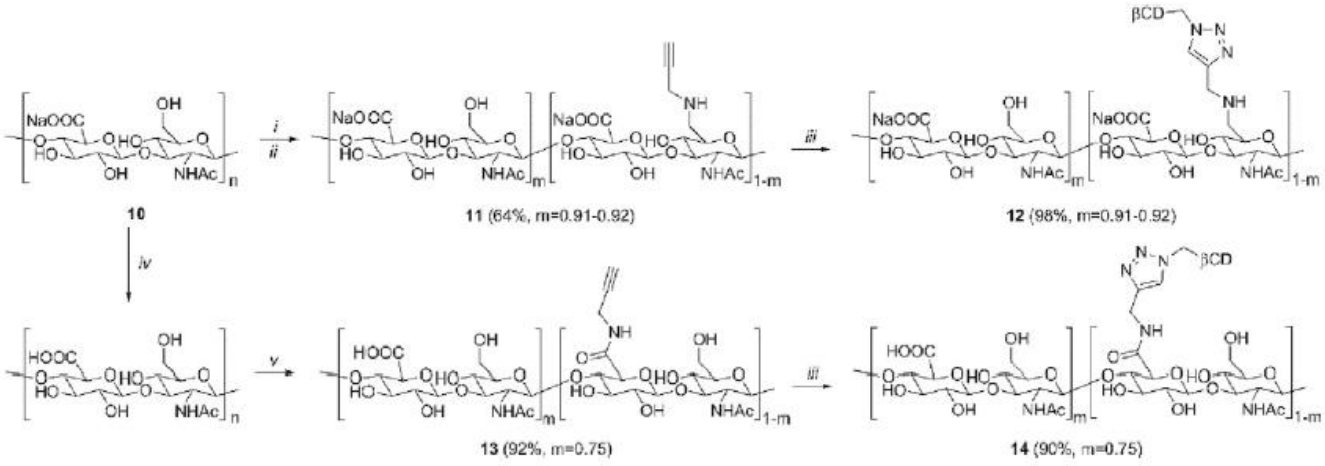

Scheme 2. Preparation of the cyclodextrin-modified HA. i 4-AcNH-TEMPO, NaClO, NaBr, Na_2HPO_4*12H_2O; ii 1) propargylamine hydrochloride, 2) 2-MePy-BH_3; iii β-CD-N_3, $CuSO_4$, sodium L-ascorbate, PBS; iv DOWEX 50WX4, H_2O; v 1) ECF, TEA, 2) propargylamine, DMSO.

The propargyl group was introduced to the HA structure in two different manners. First, C6 was modified at the N-acetylglucosamine unit via a sequence of oxidation and reductive amination. These steps were carried out in one pot since the isolation of oxidised HA intermediate and subsequent reductive amination did not lead to better results. The highest degree of oxidation calculated from ^{1}H NMR spectra and independently verified by acid-base titration (Zhao & Heindel, 1991) was about 8 %. This degree of modification was maintained in the subsequent reductive amination step. Second, propargyl amide at the glucuronic acid unit was simultaneously prepared via ethyl chlor-oformate (ECF) activation of the acidic form of HA (Huerta-Angeles et al., 2011). The approach using ECF reached a higher degree of substitution (DS, 25 %) compared with the reductive amination method (8 %).

The final step in both approaches mentioned above was a 1,3-dipolar cycloaddition of azido-CD 9 to propargylated HA. The degree of substitution was calculated from integral intensities of triazole and acetyl signals in ^{1}H NMR spectrum. DS was essentially maintained during the final step, whereas the molecular weight of the final CD-HA was significantly decreased in the case of the amide derivative 14. Successful covalent linking between CD units and the HA backbone was qualitatively indicated by an NMR DOSY (Johnson, 1999). This experiment can separate the NMR signals of mixture components by their differences in molecular translational diffusion. Simply, heavy and/or large molecules can be distinguished from light and/or small molecules by comparison of their diffusion coefficient D (y-axis

in DOSY spectrum). Testing a product of the reaction between low-molecular-weight cyclodextrin and polymer backbone, the covalent linkage between the components is supported by observing one D value for all signals, as Fig. S21 shows for CD-HA 12, in contrast to a physical mixture of two components (spectrum would be divided into two lines).

2.2. Cytotoxicity of the tritopic guests 6a-6e and polymers CD-HA 12 and 14

Since the supramolecular systems are intended for bioengineering applications, all components (compounds 6a-6e and both polymers CD-HA 12 and 14) were routinely tested for biocompatibility. In vitro cytotoxicity evaluation represents the first stage of chemical compounds or other biomaterials tested. This experiment aims to show the possible cytotoxic effect of chemical compounds or products. According to the standard ISO 10993-5, cells were incubated with sample solutions and their cytotoxicity was determined by MTT assay: a rapid and effective method for mitochondrial damage testing that correlates well with cell proliferation. Samples with cell viability >70 % are considered noncytotoxic. The results of cytotoxicity testing are presented in Fig. 1. As seen, determining the cytotoxicity of the 6a-6e, 12 and 14 samples against NIH/3T3 mouse embryonic fibroblasts did not show any significant negative impact on cell culture.

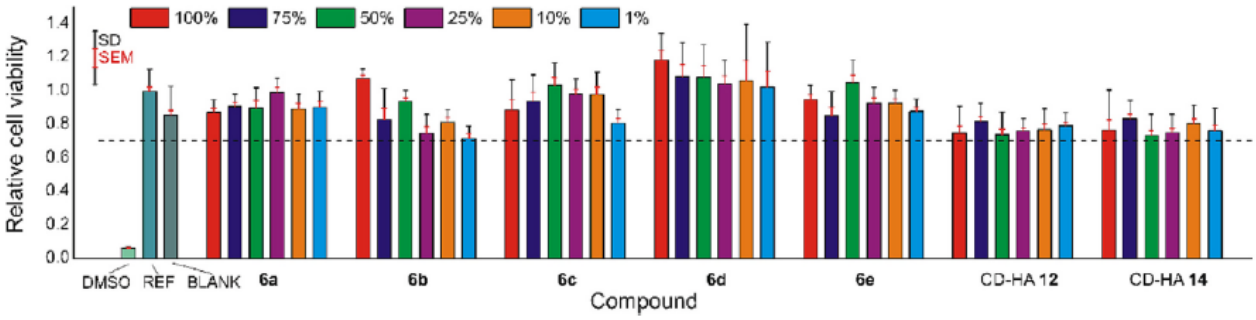

Fig. 1. Viability of the NIH/3T3 cell line after exposure to compounds 6a-6e and CD-HA 12 and 14 for 24 h. Dilution of the initial solutions is given in percentage SD and SEM indicate the standard deviation and standard error of the mean, respectively. The dashed line y = 0.7 represents the cytotoxicity threshold.

2.3. Verification of the supramolecular network

^{1}H NMR titration experiments were used to verify if CD-HA polymers are able to bind adamantane-based guests. Initially, tritopic guests 6a-6e were titrated with natural β-CD to describe supramolecular behaviour of these compounds. As seen in Fig. 2B, the H-atoms of the adamantane cage were deshielded with increasing portions of β-CD in the mixture. This behaviour is typical for an adamantane cage being complexed inside a β-CD cavity (Schneider et al., 1998). A ROESY experiment was also performed on the final mixture. Cross-peaks, which are clearly seen in Fig. S22, indicate spatial proximity of H-atoms from the β-CD cavity interior and H-atoms of the adamantane cage. Similarly, a titration with polymer CD-HA 12 was performed to observe comparable deshielding of adamantane H-atoms (Fig. 2A). Therefore, it is inferred that the polymer CD-HA 12 can interact with adamantane-based cross-linking agents to form a supramolecular network. In addition, the complexation ability of

CD-HA 12 and 14 was verified independently using titration calorimetry (ITC). A standard single-site guest (Tomecek et al., 2021) displaying an extraordinarily high affinity towards β-CD was used to demonstrate that, essentially, all CD units at CD-HA polymers are available for complexation. Results are given in SI (Fig. S25).

2.4. Rheological studies

In the formulation of supramolecular networks using multitopic constituents, the accurate ratio of the components plays a crucial role. If there is an excess of a host component, the cross-linking potential of the system is not fully employed. An excess of guest motifs leads to the oversaturation of the system. Thus, any deviation from an optimal ratio decreases the number of cross-linking points to worsen the network properties. Considering the parameters of the prepared CD-HA 12 (DS and Mw) and the adamantane-based cross-linkers 6a-6e (Mw), five mixtures were prepared to contain variable portions of cyclodextrin and adamantane units. The viscosity of these mixtures was determined using rotational rheometry to verify the correct molar ratio of the components. In order to suppress the adverse effects of thermal motion, the measurement was conducted at a low temperature (288 K).

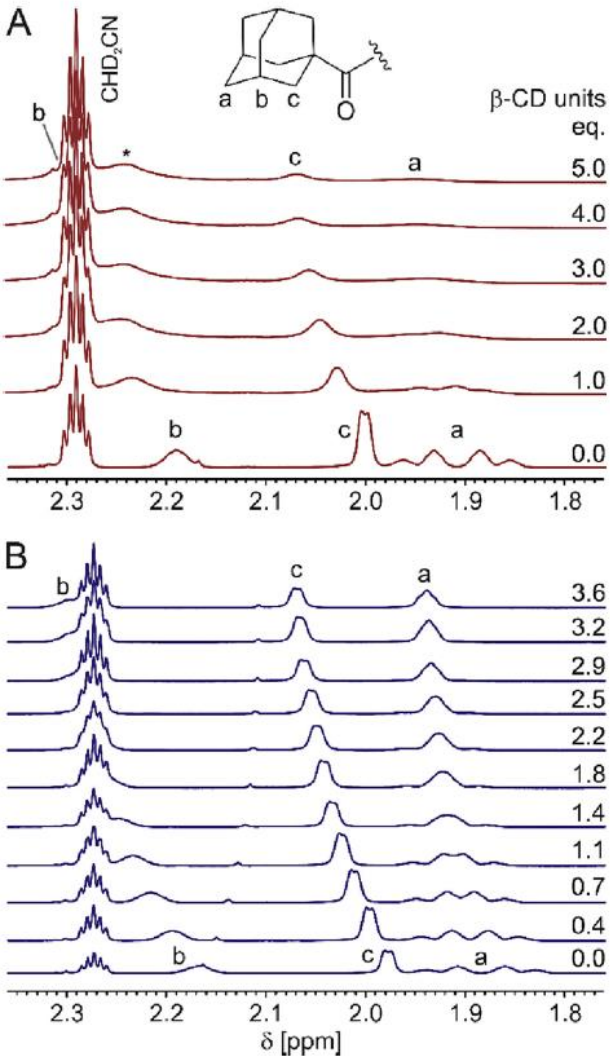

Fig. 2. ^{1}H NMR titration of the tritopic guest 6a (initial concentration 0.92 mM) with CD-HA 12 (A) and β-CD (B) (D_2O:CD_3CN, 2:1, v:v; 303 K). The signal of -HN-$COCH_3$ is labeled with an asterisk.

The results for HA 12 (4 % in H2O:MeCN, 4:1, v:v) and tritopic guest 6c is shown in **Fig. 3.** The maximal viscosity, indicating the maximal number of crosslinking points, clearly matches the theoretically optimal 1:1 ratio of the CD and Ad units, which was maintained for further experiments.

Next, the supramolecular network formation capabilities of CD-HA 12 and 14 were compared. As mentioned above, polymer 12 displays significantly lower DS than polymer 14 (8 % versus 25 %), but the average weight of polymer chains was higher in the case of 12. It can be easily calculated that polymers 12 and 14 have approximately 18 and 10 CD units per average chain, respectively. A series of samples containing 6 % CD-HA 12 and 8 % CD-HA 14 in water and the corresponding optimal amount (see above) of each compound 6a-6e (in MeCN) was prepared to carry out oscillation rheometry. Oscillation, rather than rotation, was chosen in order to follow viscoelastic properties - complex viscosity, storage and loss moduli - allowing the elastic response of the materials to be characterised.

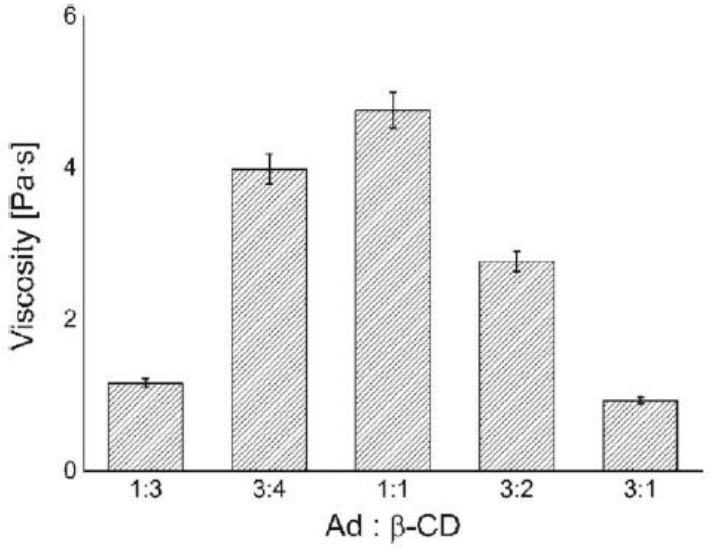

Fig. 3. Dependence of viscosity on component ratio for mixtures of CD-HA 12 and tritopic guest 6c.

This is a crucial point to confirm the effective formation of supramolecular cross-links. The dependence of storage and loss moduli on angular frequency revealed that a supramolecular 3D network was formed to a certain extent in almost all the prepared mixtures (Fig. 4), as the elastic exceeded the viscous response at low frequencies. Thus, it can be concluded that almost all the systems match a definition of the gel having a damping factor of < 1 (Fig. 5). Damping factor - the ratio of loss modulus to storage modulus - characterises the viscous to elastic response of the material. By definition, liquids have damping factor > 1, as the loss modulus exceeds storage modulus. Damping factor < 1, on the other hand, indicates solid character of the measured substance. Therefore, Fig. 5 clearly shows that samples formed of CD-HA 14 behave more liquid-like compared to their CD-HA 12 counterparts, suggesting a superior potential to form supra-molecular networks in the latter case. This can be clearly seen again in Fig. 4, where the mixtures show crossover of loss and storage moduli in all mixtures, indicating the transition from a solid to liquid state at high angular frequencies within the measured range. This behaviour is consistent with the non-covalent character of supramolecular bonding, which may provide a sensitive response to applied shear stress.

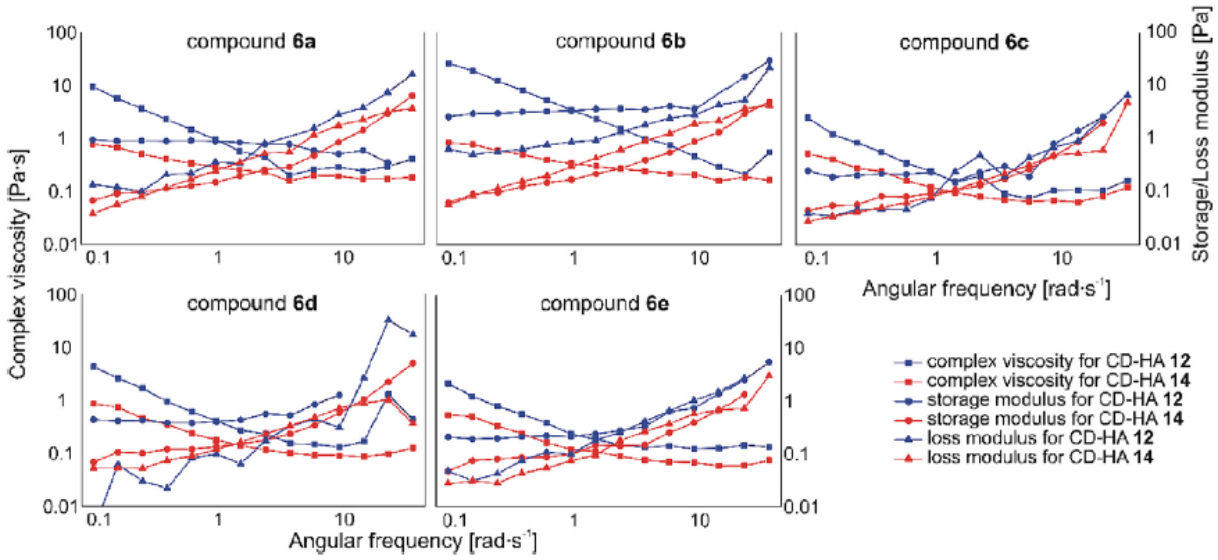

Fig. 4. Dependence of viscoelastic properties - complex viscosity (squares), storage (circles) and loss (triangles) moduli - on angular frequency in oscillation for compounds 6a-6e with CD-HA 12 (6 %, solid blue lines) and CD-HA 14 (8 %, red dashed lines). (For interpretation of the references to colour in this figure legend, the reader is referred to the web version of this article.)

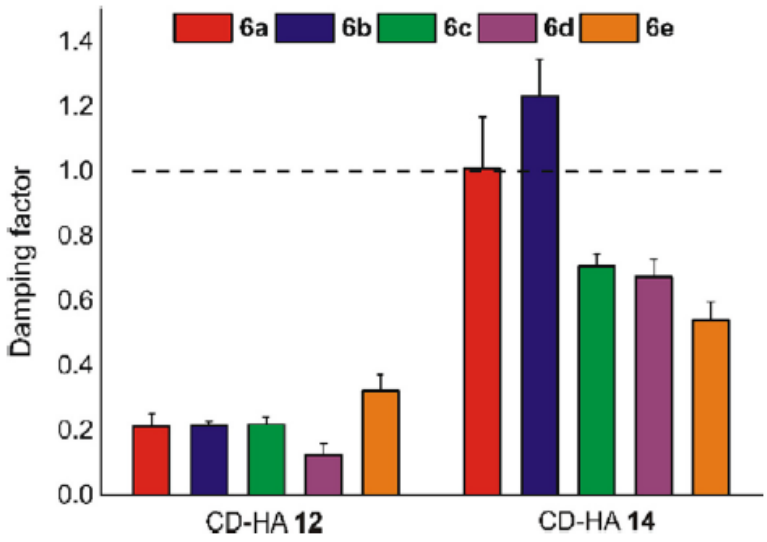

Fig. 5. Damping factor (averaged within angular frequencies 0.1-1 rad.s $^{-1}$) of mixtures 6 % CD-HA 12 and 8 % CD-HA 14 with tritopic guests 6a-6e in H_2O: MeCN (4:1; v:v).

As seen in **Fig. 6**, complex viscosities of the mixtures with CD-HA 14 samples were observed under 1 Pa-s in all cases, whereas the samples containing the CD-HA 12 showed a complex viscosity of one to two orders of magnitude higher (for full data, see Figs. S26 and S27), despite the lower polymer concentration.

Complex viscosity (Fig. 6) indicates higher mechanical stability of samples utilising 6 % solution of CD-HA 12, confirming the assumptions made based on the results of the damping factor. According to these data, it can also be assumed that Mw of modified biopolymer is a more important factor than DS to achieve desirable viscoelastic properties. Due to unsatisfactory results for CD-HA 14, this polymer was excluded from further experiments. In addition, the tritopic linkers 6b and 6a, which contain three and six N-atoms in their structure, respectively, provided significantly improved viscoelastic properties compared to their ester-based analogues. It can be hypothesised that the nature of cross-linking agents (amide versus ester) plays a more important role than the length of the arm (all of them are significantly shorter with respect to the length of the polymer). These systems also showed shear thinning behaviour (Fig. 4) and a significant increase of both complex viscosity and storage modulus in comparison to blank (for more details, see Fig. S28). Additionally, the storage modulus was independent on angular frequency within a wide frequency range, which is a clear indication of the presence of a 3D network. Thus, the ability of the proposed polymer system to facilitate formation of supramolecular gels has been confirmed.

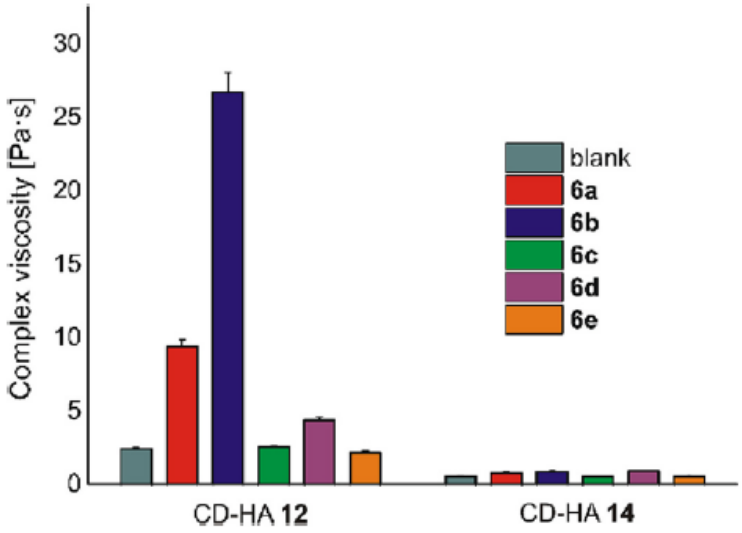

Fig. 6. Complex viscosities of mixtures 6 % CD-HA 12 and 8 % CD-HA 14 with tritopic guests 6a-6e in H_2O:MeCN (4:1; v:v).

Finally, the reversibility of the formation of the supramolecular network was tested. Since the process of gelation in physically cross-linked systems is driven by non-covalent interactions, spontaneous, rapid and full recovery of the supramolecular network should be achieved after disruption via external stimuli (e.g. shear stress, temperature). Therefore, the prepared cross-linked HA systems were subjected to cyclic shear stress. Fig. 7 shows a typical result for the compound 6b. It is clear that complex viscosity of the system is fully reversible, as it returns to the initial values after reversing the angular frequency through the crossover point. This behaviour clearly demonstrates the reversibility of the networks and indicates self-healing properties of the supramolecular bonds.

3. Conclusion

In conclusion, a series of C_{3h} star-like tritopic cross-linking agents bearing adamantane moieties (6a-6e) was synthesised successfully. The molecules of these compounds differ in the number of ethylene glycol units and the nature of amide or ester linkages between the central unit, arms and terminal adamantane binding motifs.

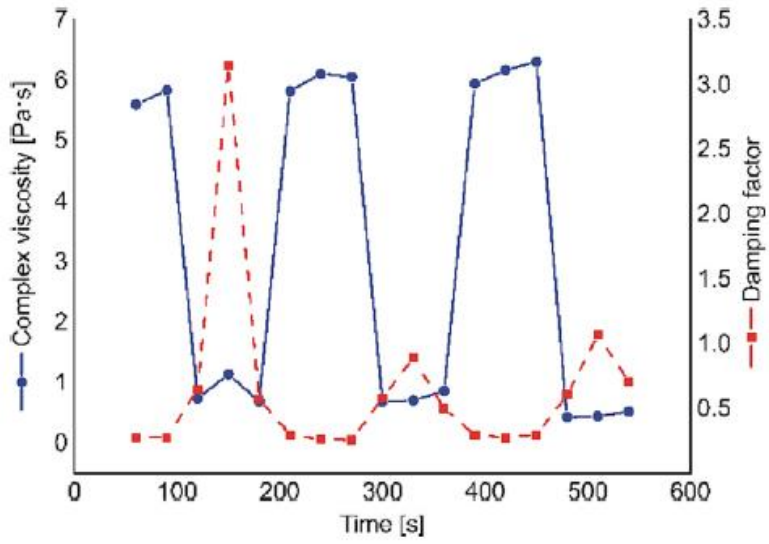

Fig. 7. Cyclic shear force test on the mixture of 6 % CD-HA 12 and tritopic guests 6b.

Two original hyaluronan polymers (CD-HA) were also prepared, and their chains were modified with β-cyclodextrin in two manners at the C6 position of either the N-acetylglucosamine (polymer 12, amine linkage, 8 % DS) or glucuronic acid (polymer 14, amide linkage, 25 % DS) subunit. All compounds 6a-6e and CD-HA 12 and 14 were found to be non-cytotoxic using standard cytotoxicity tests on mouse embryonic fibroblasts. Mixing CD-HA with cross-linking agents led to the formation of a 3D supramolecular network based on the complexation of adamantane motifs inside the CD's cavities. These host-guest complexes were confirmed by :H NMR titration experiments. Subsequently, the supramolecular 3D networks were described using rheological measurements. Based on these data, we can conclude that CD-HA 12 (DS 8 % and Mw = 105 kDa) provided significantly better viscoelastic properties than CD-HA 14 (DS 25 % and Mw = 26 kDa). The data further indicate significant differences between respective cross-linking agents. The best viscoelastic properties were achieved in the case of mixtures of tritopic guests containing at least one amide linkage per arm (i.e. 6a, 6b) with 6 % aqueous solution of CD-HA 12.

This study demonstrated the reversibility of the formation of a su-pramolecular network and hence a self-healing property of the 3D su-pramolecular frameworks via the application of cyclic shear stress. The initial hypothesis that multitopic low-molecular-weight guests can act as modular cross-linking agents, allowing for tuning of the physical properties of the supramolecular network, was verified. Consequent studies regarding the improvement of the mechanical properties to achieve printable gels are in progress.

4. Experimental section

4.1. General

All solvents, reagents and starting compounds (if not mentioned otherwise) were of analytical grade, purchased from commercial sources and used without further purification. Column chromatography was carried out on silica gel (Merck, USA, NJ; grade 60, 70-230 mesh). Reactions, the course of separation and the purity of substances were monitored by TLC Alugram® SIL G/UV_{254} foils (Macherey-Nagel, Germany). We obtained HA of 124 kDa and 600 kDa from Contipro Inc., Dolni Dobrouc, Czech Republic.

NMR spectra were recorded using a Jeol JNM-ECZ400R/S3 spectrometer operating at frequencies of 399.78 MHz for 1H and 100.53 MHz for ^{13}C. ^{1}H and ^{13}C NMR chemical shifts were referenced to the signal of the solvent [^{1}H: δ(residual $CHCl_3$) = 7.27 ppm; ^{13}C: δ($CDCl_3$) = 77.0 ppm]. Signal multiplicity is indicated by 's' for singlet, 't' for triplet, 'm' for multiplet and 'um' for unresolved multiplet. The values of coupling constants were determined by Peak Fitting function in ACD/NMR Processor Academic Edition, and spectra were processed using a DELTA v6.1 software. All spectra were recorded at 303 K. ROESY parameters were as follows: 4 scans, mixing time 400 ms, spinlock strength 3 kHz. DOSY (bpp_led_dosy_pfg JEOL pulse sequence) parameters were as follows: 16 scans, gradients 20-852 $mT \cdot m^{-1}$ in 52 $mT \cdot m^{-1}$ steps, τ = 3 ms, diffusion time = 150 ms, Δ = 5 ms, g = 3 $mT \cdot m^{-1}$.

The **IR spectra** were recorded using KBr discs with an ALPHA-T FT-IR spectrometer (Bruker Optics, Ettlingen, Germany), and $\tilde{\nu}$ was reported in cm^{-1}. Signal intensity is indicated by 's' for strong, 'm' for medium, 'w' for weak and 'br' for a broad signal.

The electrospray mass spectra (ESI-MS) of single guests or their mixtures with inorganic salts (LiCl, KCl, CsCl, $MgCl_2$, $CaCl_2$ and $BaCl_2$) were recorded using an amaZon X ion-trap mass spectrometer (Bruker Daltonics, Bremen, Germany) equipped with an electrospray ionisation source. All the experiments were conducted in positive-ion polarity mode. The single guest (with concentrations of 0.5 $\mu g \cdot cm^{-3}$) or its mixture with corresponding inorganic salt (2.5 µM) was infused into the ESI source in MeOH:H_2O (1:1, v:v) solution using a syringe pump with a constant flow rate of 0.003 $cm^3 \cdot min^{-1}$. The other instrumental conditions were as follows: an electrospray voltage of — 4.2 kV, a capillary exit voltage of 140 V, a drying gas temperature of 493 K, a drying gas flow rate of 6.0 $dm^3 \cdot min^{-1}$ and a nebuliser pressure of 55.16 kPa. Nitrogen was used as both the nebulising and drying gas for all the experiments. Tandem mass spectra were collected using collision-induced dissociation with He as the collision gas after the isolation of the required ions.

Isothermal titration calorimetry (ITC) measurements were carried out in H_2O using a VP-ITC MicroCal instrument at 303 K. The concentrations of the host in the cell (CD-HA 12 and CD-HA 14) and the standard guest in the microsyringe (1Ad, for structure, see Fig. S25) were approximately 0.10 mM and 1.00 mM. The heats of dilution were considered for each measurement. The raw experimental data were analysed with the MicroCal ORIGIN software. The data were fitted to a theoretical titration curve using the 'One Set of Sites' model.

Gel permeation chromatography (GPC): The average molecular weight and distribution curve of hyaluronan and its derivatives were determined by GPC performed on a high-performance liquid chromatograph system Shimadzu Prominence (Shimadzu, Japan) equipped with a refractive index (RI) detector (Shimadzu Prominence, LC-20 series, Shimadzu, Japan). The conditions of analysis were as follows: 0.1 M PBS solution with pH = 7.4, flow = 0.8 $cm^3 \cdot min^{-1}$, oven temperature = 303 K. PL aqua gel-OH 60 columns (8 µm, 300 x 7.5 mm) and PL aqua gel-OH 40 (8 µm, 300 x 7.5 mm) were connected in series. Pullulan standards (Mw = 805; 348; 200; 113; 48.8; 21.7; 10; 6.2; 1.32; 0.342 kDa; PSS GmbH, Germany) were used for molecular weight calibration. The concentration of prepared samples was 2.5

mg/cm^3. Each sample was filtered through a nylon 0.45 µm syringe filter (13 mm diameter). The sample injection volume was 0.01 cm^3. Data were processed using LabSolutions GPC Software (Shimadzu, Japan).

Cytotoxicity testing was done according to ISO standard 10993 using the NIH/3T3 cell line. The NIH/3 T3 cell line derived from mouse embryonic fibroblasts (ATCC CRL-1658 NIH/3 T3, USA) was maintained in the Dulbecco's Modified Eagle's Medium (BioSera, France) containing 10 % bovine calf serum (BioSera, France) and 1 % of Penicillin/Strep-tomycin (GE Healthcare HyClone, United Kingdom) as a cultivation medium at standard conditions 37 °C in 5 % CO_2 in humidified air.

For in vitro cytotoxicity testing, ISO 10993-12 defines the reference materials used in the former, while ISO 10993-5 establishes the test procedures. Sample specimens were prepared in accordance with ISO 10993-12 with the specified protocol. The samples were sterilised using UV light, and an appropriate amount of UPW was added for dissolution. A solution of β-CD was then pipetted to the samples and the real solutions were shaken for 24 h. This ensured the maximum possible dissolution. Next, the tested solution was incubated in a cultivation medium for 24 h at 310 K with stirring. Subsequently, the extracts were filtered using a syringe filter with a pore size of 0.22 µm. One day before the exposition, cells were trypsinised and resuspended in a medium to create a suspension with a concentration of 1 x 10^5 cells per cm^3. Thereafter, 0.1 cm^3 of the cell suspension was seeded into a 96-well plate (TPP, Trasadingen, Switzerland). The parent extracts were then diluted in a medium to obtain a series of dilutions with concentrations of 75, 50, 25, 10 and 1 vol%. The filtered samples in the required dilutions were added to the cells and incubated for 24 h. To determine cell viability, tetra-zolium salt (MTT cell proliferation assay kit, Duchefa Biochemie, Netherlands) was used. The MTT test was performed according to ISO 10993-5: Appendix C. Absorbance was measured using a microplate reader, Infinite M200 PRO (Tecan, Männedorf, Switzerland) at 570 nm, and the reference wavelength was adjusted to 690 nm. The results are presented as the relative cell viability compared to the reference (cells cultivated without samples), which corresponds to 1 (meaning 100 % cell viability). The β-CD solution was used as a blank. The morphology of cells from the culture plates was observed using an inverted Olympus phase-contrast microscope (IX 81) (Olympus, Germany).

Rheometry. All measurements were performed using a rotational rheometer, Anton-Paar MCR 502 (Anton-Paar, Gratz, Austria) at 15 °C or 25 °C, respectively, under normal pressure in a room atmosphere. Rheometry on supramolecular networks was performed using a Peltier measuring system P-PTD200/62/TG with PP/25. The viscosity of samples was measured in steady shear mode at a constant shear rate of 0.1 s^{-1}. On the other hand, measurement of complex characteristics (complex viscosity, storage (G') and loss (G") moduli, and damping factor (G"/G')), was done in oscillation mode at deformation corresponding to the linear region of viscosity with angular frequency sweep increasing from 0.1 to 100 rad·s^{-1}. The samples were placed in the centre of the measuring system, and the upper geometry was brought down so that the sample fills the measuring gap completely. The thickness of the sample was between 1.2 and 1.8 mm.

4.2. Syntheses

4.2.1. 1-Adamantanecarbonyl chloride (2a)

A mixture of adamantane-1-carboxylic acid (1a) (3 g; 16.6 mmol), excess of thionyl chloride ($SOCl_2$) and two drops of N,N-dime-thylformamide (DMF) was heated under reflux for 3 h affording a clear solution. The remaining $SOCl_2$ was evaporated in a vacuum to obtain the acid chloride as a white-to-yellow crystalline solid in a quantitative yield.

4.2.2. Trimesic chloride (2b)

Benzene-1,3,5-tricarboxylic acid (1b) (1 g; 4.8 mmol) was dissolved in an excess of $SOCl_2$, subsequently two drops of DMF were added and the resulting solution was refluxed for 4 h. The remaining $SOCl_2$ was removed in a vacuum to obtain the 2b as a white-to-yellow crystalline solid in a quantitative yield.

4.2.3. tert-Butyl 2-[2-(2-aminoethoxy)ethoxy]ethylcarbamate (4a)

The product was prepared according to a slightly modified, previously published procedure (Otremba & Ravoo, 2017). A solution of Boc_2O (4 g; 18.3 mmol) in 40 cm^3 of dry dichloromethane (DCM) was added dropwise into a cooled solution of diamine 3 (16.3 g; 110 mmol; 6 eq.) in dry DCM (30 cm^3) under nitrogen atmosphere within a few hours. The resulting mixture was stirred overnight at room temperature and then washed with water six times, dried over Na_2SO_4 and concentrated in a vacuum to obtain the product as a colourless liquid in 60 % yield (2.73 g; 11 mmol) with respect to Boc_2O. ^1H NMR ($CDCl_3$, 400 MHz): δ 1.25 (s, 2H), 1.38 (s, 9H), 2.81 (t, 2H), 3.25 (m, 2H), 3.45 (um, 2H), 3.49 (um, 2H), 3.55 (um, 2H), 3.56 (um, 2H), 5.17 (s, 1H) ppm. The collected data are in agreement with those previously published (Otremba & Ravoo, 2017).

4.2.4. N-{2-[2-(2-aminoethoxy)ethoxy]ethyl}-1-adamantane carboxamide (5a)

The product was prepared according to a slightly modified, previously published procedure (Samanta et al., 2015). A solution of 2a (2.7 g; 13.6 mmol; 1.3 eq.) in dry DCM (30 cm^3) was added dropwise into an ice-cooled solution of compound 4a (2.585 g; 10.4 mmol; 1 eq.) and triethylamine (TEA) (8.7 cm3; 62.5 mmol; 6 eq.) in dry DCM (25 cm3). The resulting mixture was stirred overnight at room temperature and then washed twice with 1 M K2CO3, once with brine, dried over Na2SO4 and concentrated in a vacuum to obtain a yellow oil, which was used without further purification and characterisation.

A solution of this yellow oil in DCM (10 cm^3) and trifluoroacetic acid (TFA, 5 cm3) was stirred at room temperature for 3 h and then concentrated in a vacuum. The residue was suspended in 10 % NaOH solution and extracted with DCM. The organic phase was washed with NaOH again, water, brine and dried over Na_2SO_4 and concentrated in a vacuum to obtain 5a as a red oil in 94 % yield (3.03 g; 9.76 mmol) with respect to 4a. ^1H NMR ($CDCl_3$, 400 MHz): δ 1.39 (s, 2H), 1.70 (um, 6H), 1.83 (um, 6H), 2.01 (um, 3H), 2.86 (m, 2H), 3.42 (m, 2H), 3.50 (m, 2H), 3.53 (m, 2H), 3.60 (um, 4H), 6.01 (s, 1H) ppm. The collected data are in agreement with those previously published (Samanta et al., 2015).

4.2.5. N-[2-(2-hydroxyethoxy)ethyl]-1-adamantane carboxamide (5b)

The product was prepared according to a slightly modified, previously published procedure (Korosec et al., 1992). A solution of 2a (1.2 g; 6 mmol) in dry DCM (5 cm^3) was added dropwise into an ice-cooled solution of 2-(2-aminoethoxy)ethanol (4b) (2.4 cm^3; 24 mmol; 4 eq.) in dry DCM (10 cm^3). The resulting mixture was stirred overnight at room temperature and then washed four times with 1M HCl, once with brine, dried over Na_2SO_4 and concentrated in a vacuum. A pure 5b was obtained as a colourless oil in 76 % yield (1.23 g; 4.6 mmol) with respect to 2a. ^1H NMR ($CDCl_3$, 400 MHz): δ 1.72 (um, 6H), 1.85 (um, 6H), 2.04 (um, 3H), 3.46 (m, 2H), 3.56 (m, 2H), 3.58 (m, 2H), 3.75 (m, 2H) ppm. $^{13}C\{^1H\}$ NMR ($CDCl_3$, 101 MHz): δ 28.1, 36.5, 39.0, 39.2, 40.6, 61.7, 70.0, 72.1, 178.2 ppm. The collected data are in agreement with those previously published (Korosec et al., 1992).

4.2.6. 2-(2-Hydroxyethoxy)ethyl-1-adamantane carboxylate (5c)

A solution of 2a (1.2 g; 6 mmol) in dry DCM (5 cm^3) was added dropwise into an ice-cooled solution of diethylene glycol (4c) (1.147 cm^3; 12 mmol; 2 eq.) and TEA (1.01 cm^3; 7.2 mmol; 1.2 eq.) in dry DCM (10 cm^3). The resulting mixture was stirred overnight at room temperature and then washed three times with 10 % $NaHCO_3$, once with brine, dried over Na_2SO_4 and concentrated in a vacuum. Purification by column chromatography on silica gel (EtOAc; monitored by TLC, R_f = 0.7; stained with iodine) gave pure 5c as a colourless oil in 70 % yield (1.135 g; 4.23 mmol) with respect to 2a. ^{1}H NMR ($CDCl_3$, 400 MHz): δ 1.72 (um, Ha), 1.91 (um, Hc), 2.02 (um, Hb), 3.61 (m, Hg), 3.71 (m, He), 3.74 (m, Hf), 4.23 (m, Hd) ppm. $^{13}C\{^1H\}$ NMR ($CDCl_3$, 101 MHz): δ 27.9 (Cb), 36.5 (Ca), 38.8 (Cc), 40.7 (Cca), 61.8 (Cf), 63.1 (Cd), 69.2 (Ce), 72.2 (Cg), 177.6 (Ccb) ppm. IR (KBr): 3441 (br m), 2907 (s), 2853 (s), 1728 (s), 1454 (m), 1324 (w), 1269 (m), 1236 (s), 1134 (m), 1104 (m), 1079 (s) cm^{-1}. ESI-MS (pos.) m/z (%): 559.2 $[2{\cdot}M + Na^+]^+$ (87 %), 422.1 $[3M + H^+ + K^+]2^+$ (10 %), 291.0 $[M + Na^+]^+$ (100 %).

4.2.7. 2-[2-(2-Hydroxyethoxy)ethoxy]ethyl-1-adamantane carboxylate (5d)

The product was prepared according to a slightly modified, previously published procedure (Facchin et al., 2017). A solution of 2a (6.61 g; 33.3 mmol) in dry DCM (25 cm^3) was added dropwise into an ice-cooled solution of triethylene glycol (4d) (8.883 cm3; 66.6 mmol; 2 eq.) and TEA (5.57 cm^3; 40 mmol; 1.2 eq.) in dry DCM (25 cm^3). The resulting mixture was stirred overnight at room temperature and then washed three times with 10 % $NaHCO_3$, once with brine, dried over Na_2SO_4, and concentrated in a vacuum. Purification by column chromatography on silica gel (EtOAc; monitored by TLC, R_f = 0.6, stained with iodine) gave pure 5d as a colourless oil in 61 % yield (6.315 g; 20.2 mmol) with respect to 2a. ^{1}H NMR ($CDCl_3$, 400 MHz): δ 1.72 (um, 6H), 1.91 (um, 6H), 2.02 (um, 3H), 2.23 (s, 1H), 3.62 (m, 2H), 3.67 (um, 4H), 3.70 (m, 2H), 3.74 (m, 2H), 4.22 (m, 2H) ppm. $^{13}C\{^1H\}$ NMR ($CDCl_3$, 101 MHz): δ 27.9, 36.5, 38.8, 40.7, 61.8, 63.1, 69.3, 70.5, 70.7, 72.5, 177.6 ppm. The collected data are in agreement with those previously published (Facchin et al., 2017).

4.2.8. 2-{2-[2-(2-Hydroxyethoxy)ethoxy]ethoxy}ethyl-1-adamantane carboxylate (5e)

The product was prepared according to a slightly modified, previously published procedure (Jiang et al., 2018). A solution of 2a (1.2 g; 6 mmol) in dry DCM (5 cm^3) was added dropwise into an ice-cooled solution of tetraethylene glycol (4e) (2.085 cm^3; 12 mmol; 2 eq.) and TEA (1.01 cm^3; 7.2 mmol; 1.2 eq.) in dry DCM (10 cm^3). The resulting mixture was stirred overnight at room temperature and then washed three times with 10 % $NaHCO_3$, once with brine, dried over Na_2SO_4 and concentrated in a vacuum. Purification by column chromatography on silica gel (EtOAc; monitored by TLC, R_f = 0.4, stained with iodine) gave pure 5e as a colourless oil in 56 % yield (1.2 g; 3.37 mmol) with respect to 2a. ^{1}H NMR ($CDCl_3$, 400 MHz): δ 1.72 (um, 6H), 1.91 (um, 6H), 2.02 (um, 3H), 3.62 (m, 2H), 3.67 (m, 4H), 3.68 (um, 4H), 3.69 (m, 2H), 3.73 (m, 2H), 4.22 (m, 2H) ppm. $^{13}C\{^1H\}$ NMR ($CDCl_3$, 101 MHz): δ 28.0, 36.6, 38.9, 40.8, 61.9, 63.3, 69.4, 70.5, 70.7, 70.8, 72.5, 77.2, 177.7 ppm. The collected data are in agreement with those previously published (Jiang et al., 2018).

4.2.9. N^1,N^3,N^5-tris(2-{2-[2-(adamantane-1-carboxamido)ethoxy] ethoxy}ethyl)benzene-1,3,5-tricarboxamide (6a)

A solution of 2b (0.983 g; 3.7 mmol) in dry DCM (15 cm^3) was added dropwise into an ice-cooled solution of 5a (3.79 g; 12.2 mmol; 3.3 eq.) and TEA (1.86 cm^3; 13.3 mmol; 3.6 eq.) in dry DCM (15 cm^3). The resulting mixture was stirred overnight at room temperature and then washed with 10 % $NaHCO_3$, dried over Na_2SO_4 and concentrated in a vacuum. Purification by column chromatography on silica gel (EtOAc: EtOH, 3:1, v:v; monitored by TLC, R_f = 0.35) gave pure 6a as a colourless semi-solid in 62 % yield (2.5 g; 2.3 mmol) with respect to 2b. ^{1}H NMR ($CDCl_3$, 400 MHz): δ 1.64 (um, Ha_{eq}), 1.71 (um, Ha_{ax}), 1.81 (m, Hc), 1.99 (um, Hb), 3.38 (q, He, $^3J_{H,H}$ = 5.4 Hz), 3.55 (t, Hf, $^3J_{H,H}$ = 5.3 Hz), 3.60 (um, Hg), 3.63 (um, Hh), 3.65 (um, Hj), 3.66 (um, Hi), 6.22 (t, Hd, $^3J_{H,H}$ = 5.4 Hz), 7.33 (um, Hk), 8.45 (s, Hl) ppm. ^{13}C {^{1}H} NMR ($CDCl_3$, 101 MHz): 8 28.1 (Cb), 36.5 (Ca), 39.0 (Cd), 39.2 (Cc), 40.0 (Ci), 40.6 (Cca), 69.5 (Ch), 69.8 (Ce), 70.1 (Cg), 70.3 (Cf), 128.5 (Cj), 135.1 (Cib), 166.0 (Cia), 178.4 (Ccb) ppm. IR (KBr): 3351 (m), 3076 (w), 2904 (s), 2850 (s), 1640 (s), 1534 (s), 1452 (m), 1288 (m), 1134 (m), 1105 (m), 742 (w) cm^{-1}. ESI-MS (pos.) m/z (%): 1125.6 $[M + K^+]^+$ (5 %), 1109.7 $[M + Na^+]^+$ (100 %), 1106.6 $[2{\cdot}M + H^+{+}K^+]^{2+}$ (7 %), 1087.7 $[M + H^+]^+$ (11 %), 566.3 $[M + 2{\cdot}Na^+]^{2+}$ (18 %), 563.3 $[M + H^+{+}K^+]^{2+}$ (17 %), 555.3 $[M + H^+{+}Na^+]^{2+}$ (11 %).

4.2.10. Tris{2-[2-(adamantane-1-carboxamido)ethoxy]ethyl}benzene-1.3.5-tricarboxylate (6b)

A solution of 2b (0.313 g; 1.18 mmol) in dry DCM (5 cm^3) was added dropwise into an ice-cooled solution of 5b (1.037 g; 3.9 mmol; 3.3 eq.) and TEA (0.59 cm^3; 4.25 mmol; 3.6 eq.) in dry DCM (10 cm^3). The resulting mixture was stirred overnight at room temperature and then washed with 10 % NaHCO3, dried over Na2SO4 and concentrated in a vacuum. Purification by column chromatography on silica gel (EtOAc: EtOH, 7:1, v:v; monitored by TLC, R_f = 0.5) gave pure 6b as colourless oil in 70 % yield (0.79 g; 0.82 mmol) with respect to 2b. ^{1}H NMR ($CDCl_3$, 400 MHz): 8 1.61 (um, Ha_{eq}), 1.69 (um, Ha_{ax}), 1.80 (um, Hc), 1.96 (um, Hb), 3.44 (q, He, $^3J_{H,H}$ = 5.3 Hz), 3.59 (t, Hf, $^3J_{H,H}$ = 5.2 Hz), 3.82 (um, Hg), 4.53 (um, Hh), 6.02 (t, Hd, $^3J_{H,H}$ = 5.4 Hz), 8.87 (s, Hi) ppm. ^{13}C {^{1}H} NMR (CDCl3, 101 MHz): δ 28.1 (Cb), 36.5 (Ca), 39.0 (Cd), 39.2 (Cc), 40.6 (Cca), 64.6 (Cg), 68.8 (Cf), 70.0 (Ce), 131.2 (Cgb), 134.7 (Ch), 164.8 (Cga), 178.0 (Ccb) ppm. IR (KBr): 3361 (m), 3085 (w), 2905 (s), 2851 (s), 1732 (s), 1640 (s), 1524 (s), 1452 (m), 1241 (s), 1136 (s), 742 (m) cm^{-1}. ESI-MS (pos.) m/z (%): 996.5 $[M + K^+]^+$ (9 %), 980.5 $[M + Na^+]^+$ (100 %), 977.5 $[2{\cdot}M + H^+{+}K^+]^{2+}$ (11 %), 958.5 $[M + H^+]^+$ (14 %), 501.7 $[M + 2{\cdot}Na^+]^{2+}$ (6 %), 498.7 $[M + H^+{+}K^+]^{2+}$ (7 %), 490.7 $[M + H^+{+}Na^+]^{2+}$ (5 %).

4.2.11. Tris(2-{2-[(adamantane-1-carbonyl)oxy]ethoxy}ethyl)benzene-1.3.5-tricarboxylate (6c)

A solution of 2b (0.417 g; 1.6 mmol) in dry DCM (5 cm^3) was added dropwise into an ice-cooled solution of 5c (1.39 g; 5.18 mmol; 3.3 eq.) and TEA (0.79 cm^3; 5.65 mmol; 3.6 eq.) in dry DCM (10 cm^3). The resulting mixture was stirred overnight at room temperature and then washed with 10 % $NaHCO_3$, dried over Na_2SO_4 and concentrated in a vacuum. Purification by column chromatography on silica gel (EtOAc: PE, 5:3, v:v; monitored by TLC, R_f = 0.8) gave pure 6c as colourless oil in 67 % yield (1.01 g; 1.05 mmol) with respect to 2b. ^{1}H NMR (CDCl3, 400 MHz): δ 1.65 (um, Haeq.), 1.70 (um, Ha_{ax}.), 1.86 (um, Hc), 1.96 (um, Hb), 3.73 (um, He), 3.85 (um, Hf), 4.22 (um, Hd), 4.53 (um, Hg), 8.88 (s, Hh) ppm. ^{13}C {^{1}H} NMR ($CDCl_3$ 101 MHz): δ 27.9 (Cb), 36.5 (Ca), 38.8 (Cc), 40.7 (Cca), 63.1 (Cd), 64.5 (Cg), 68.9 (Cf), 69.3 (Ce), 131.2 (Cgb), 134.8 (Ch), 164.9 (Cga), 177.5 (Ccb) ppm. IR (KBr): 3434 (w), 3085 (w), 2907 (s), 2852 (s), 1729 (s), 1608 (w), 1454 (m), 1325 (m), 1235 (s), 1104 (m), 1078 (s), 867 (w), 742 (m) cm^{-1} ESI-MS (pos.) m/z (%): 983.5 $[M + Na^+]^+$ (100 %).

4.2.12. Tris[2-(2-{2-[(adamantane-1-carbonyl)oxy]ethoxy}ethoxy)ethyl] benzene-1,3,5-tricarboxylate (6d)

A solution of 2b (0.330 g; 1.6 mmol) in dry DCM (5 cm^3) was added dropwise into an ice-cooled solution of 5d (1.620 g; 5.2 mmol; 3.3 eq.) and TEA (0.8 cm^3; 5.8 mmol; 3.6 eq.) in dry DCM (10 cm^3). The resulting mixture was stirred overnight at room temperature and then washed with 10 % $NaHCO_3$, dried over Na2SO4 and concentrated in a vacuum. Purification by column chromatography on silica gel (EtOAc:PE, 5:3, v: v); monitored by TLC, (R_f = 0.7) gave pure 6d as colourless oil in 80 % yield (1.37 g; 1.25 mmol) with respect to 2b. ^{1}H NMR ($CDCl_3$, 400 MHz): δ 1.70 (um, Ha), 1.88 (um, Hc), 2.00 (um, Hb), 3.70 (um, He), 3.90 (um, Hf), 3,71 (um, Hg), 3.87 (um, Hh), 4.19 (um, Hd), 4.53 (um, Hi), 8.87 (s, Hj) ppm. ^{13}C {^{1}H} NMR ($CDCl_3$, 101 MHz): δ 27.9 (Cb), 36.5 (Ca), 38.8 (Cc), 40.7 (Cca), 63.2 (Cd), 64.7 (Ci), 69.1 (Ch), 69.3 (Cf), 70.66 (Ce), 70.69 (Cg), 131.2 (Cib), 134.8 (Cj), 164.9 (Cia), 177.5 (Ccb) ppm. IR (KBr): 3430 (w), 3086 (w), 2907 (s), 2853 (s), 1729 (s), 1608 (w), 1453 (m), 1325 (m), 1237 (s), 1104 (m), 1078 (s), 865 (m), 742 (m) cm^{-1}. ESI-MS (pos.) m/z (%): 1115.6 [M + Na^+]$^+$ (100 %).

4.2.13. Tris[1-(adamantan-1-yl)-1-oxo-2,5,8,11-tetraoxatridecan-13-yl] benzene-1,3,5-tricarboxylate (6e)

A solution of 2b (0.423 g; 1.6 mmol) in dry DCM (5 cm^3) was added dropwise into an ice-cooled solution of 5e (1.87 g; 5.2 mmol; 3.3 eq.) and TEA (0.8 cm^3; 5.8 mmol; 3.6 eq.) in dry DCM (15 cm^3). The resulting mixture was stirred overnight at room temperature and then washed with 10 % $NaHCO_3$, dried over Na_2SO_4 and concentrated in a vacuum. Purification by column chromatography on silica gel (EtOAc; monitored by TLC, R_f = 0.7) gave pure 6e as a colourless oil in 53 % yield (1.04 g; 0.85 mmol) in respect to 2b. ^{1}H NMR ($CDCl_3$, 400 MHz): δ 1.69 (um, Ha), 1.87 (um, Hc), 1.99 (um, Hb), 3.62 (um, Hh), 3.63 (um, Hf), 3.66 (um, He), 3.68 (um, Hg), 3.71 (um, Hi), 3.85 (um, Hj), 4.18 (um, Hd), 4.52 (um, Hk), 8.85 (s, Hl) ppm. ^{13}C {^{1}H} NMR ($CDCl_3$, 101 MHz): δ 27.9 (Cb), 36.5 (Ca), 38.8 (Cc), 40.6 (Cca), 63.2 (Cd), 64.7 (Ck), 69.0 (Cj), 69.2 (Ce), 70.58 (Cf), 70.64 (Ch), 70.66 (Cg, Ci), 131.2 (Ckb), 134.8 (Cl), 164.9 (Cka), 177.5 (Ccb) ppm. IR (KBr): 3432 (w), 3086 (w), 2906 (s), 2854 (s), 1728 (s), 1608 (w), 1454 (m), 1325 (m), 1238 (s), 1078 (s), 865 (m), 742 (m) cm^{-1}. ESI-MS (pos.) m/z (%): 1263.6 [M + K^+]$^+$ (6 %), 1247.7 [M + Na^+]$^+$ (100 %), 635.3 [M + 2·Na^+]$^{2+}$ (26 %), 632.3 [M + H^++K^+]$^{2+}$ (10 %).

4.2.14. Mono-6-O-(p-toluenesulfonyl)-β-cydodextrin (8)

The product was prepared according to a slightly modified previously published procedure (Petter et al., 1990). An aqueous solution of NaOH (0.55 g; 5 cm^3; 13.7 mmol) was added dropwise into an ice-cooled (0 °C) suspension of 7 (5.0 g, 4.4 mmol) in 42 cm^3 of water providing a homogeneous clear solution. After warming to room temperature, p-toluenesufonyl chloride (1.01 g; 5.3 mmol; 1.2 eq.) in 2.5 cm^3 of acetonitrile was added dropwise over 5 min with the immediate formation of a colourless precipitate. After stirring for 2 h at 22 °C the precipitate was removed by suction. The filtrate was cooled in an ice bath and pH was adjusted to 3-4 with 35 % HCl; a fine colourless precipitate started to form within a few minutes and the suspension was refrigerated at 6 °C overnight. Product 8 was obtained as a colourless solid by suction and air-drying in 18 % yield (0.8 mmol, 1.03 g) with respect to 7. ^{1}H NMR (DMSO-d_6, 400 MHz): δ 2.43 (s, 3H, CH_3), 3.22-3.40 (um, 12H, P-CD H2, H4), 3.50-3.70 (um, 24H, β-CD H3, H5, H6), 4.20 (um, 1H, β-CD H5'), 4.32 (um, 2H, β-CD H6'), 4.41-4.46 (um, 6H, β-CD OH6), 4.77 (um, 1H, β-CD H1'), 4.84 (um, 6H, β-CD H1), 5.68 (um, 12H, β-CD OH2, OH3), 5.78 (um, 1H, β-CD OH2', $^3J_{H,H}$ = 6 Hz), 7.43 (um, 2H, arom.), 7.75 (um, 2H, arom.) ppm. The collected data are in agreement with those previously published (Petter et al., 1990).

4.2.15. Mono-6-azido-6-deoxy-fi-cydodextrin (9)

The product was prepared according to a slightly modified, previously published procedure (Petter et al., 1990). To 0.98 g (0.76 mmol) of 8 suspended in dry DMF (6 cm^3), 0.248 g (3.8 mmol; 5 eq.) of NaN_3 was added and the resulting mixture was heated to 75 °C, upon which the starting material dissolved. After 72 h at the elevated temperature the mixture was cooled to room temperature and quenched by pouring it into 50 cm^3 of acetone. The yellowish precipitate was filtered, dissolved in the smallest possible amount of water and precipitated again with acetone. This procedure was repeated three times to yield a fine colourless solid. The solid was dissolved in water and treated with Amberlite MB-2 resin to remove salts. The ion exchange procedure was quenched after 1 h by filtering the resin beads away. After freeze-drying, pure 9 was obtained as a colourless solid in 61 % yield (0.465 g; 0.4 mmol) with respect to 8. ^{1}H NMR (DMSO-d_6, 400 MHz): δ 3.33 (um, 6H, β-CD H2), 3.39 (um, 6H, β-CD H4), 3.57 (um, 6H, β-CD H5), 3.64 (um, 6H, β-CD H3), 3.66 (um, 12H, β-CD H6), 3.77 (um, 1H, β-CD H5'), 4.42 (um, 6H, β-CD OH6), 4.49 (um, 2H, β-CD H6'), 4.83 (um, 6H, β-CD H1), 4.88 (um, 1H, β-CD H1', $^3J_{H,H}$ = 3.5 Hz), 5.60 (um, 1H, β-CD OH3', $^3J_{H,H}$ = 2.4 Hz), 5.68 (um, 6H, OH3), 5.72 (um, 6H, OH2) ppm. The collected data are in agreement with those previously published procedure (Petter et al., 1990).

4.2.16. Propargylamino-HA (11)

The product was prepared according to a slightly modified, previously published procedure (Huerta-Angeles et al., 2012; Šedova et al., 2013). Sodium hyaluronate (10; 124 kDa; 1.1 g) was left to dissolve in 73 cm^3 of water overnight. Into the resulting viscous solution was added NaBr (0.212 g; 2.1 mmol; 0.75 eq.) and $Na_2HPO_4 \cdot 12\ H_2O$ (1.21 g; 3.4 mmol; 1.23 eq.), then it was cooled in an ice-bath to 0-5 °C and bubbled with nitrogen before 4-acetamido-TEMPO (5.86 mg; 0.03 mmol; 0.01 eq.) was added. Subsequently, sodium hypochlorite (1.34 cm^3 of 4.9 % aqueous solution) was added, and an oxidation reaction was carried out for 20 min. The reaction was then quenched by the addition of glacial acetic acid to pH = 5. Upon the addition of propargyl amine hydrochloride (0.4 g; 4.36 mmol; 2.3 eq.) the mixture was stirred for an additional 5 h. The imine thus formed was then reduced by picoline borane (90 mg; 0.84 mmol; 0.3 eq.) added to the solution, and the reaction continued overnight. The product was purified by dialysis (cut-off 14 kDa) against a solution of 0.1 % NaCl and 0.1 % $NaHCO_3$ (3 x 8 dm^3) and demineralised water (6 x 8 dm^3). After freeze-drying, pure 11 was obtained in 64 % yield (0.76 g; DS = 8-9 %; Mw = 79 kDa). ^{1}H NMR (NaOD in D_2O, 400 MHz): δ 1.89 (um, 3H, NHAc), 2.75 (m, CH_2), 3.00 (m, CH_2), 3.36 (um, HA), 3.50 (um, HA), 3.64 (um, HA), 3.86 (um, HA), 4.38 (um, 1H, HA), 4.47 (um, 1H, HA) ppm. The collected data are in agreement with those previously published (Huerta-Angeles et al., 2012).

4.2.17. β-Cyclodextrin modified propargylamino-HA (12)

The product was prepared according to a slightly modified, previously published procedure (Kovacevic et al., 2019). Propargylamino-HA 11 (0.51 g; 1.25 mmol; DS = 8-9 %; Mw = 79 kDa) was dissolved in 25 cm^3 of 0.1 M phosphate-buffered saline solution (PBS; pH 7.4). Subsequently, solid compound 9 (0.23 g; 0.2 mmol), $CuSO_4 \cdot 5H_2O$ (0.02 g; 0.08 mmol) and sodium ascorbate (0.02 g; 0.1 mmol) were added to the solution. The reaction mixture was then stirred vigorously overnight at room temperature. The product was purified by dialysis (cut-off 14 kDa) against 0.01 % EDTA (2 x 8 dm^3) and then against water (6 x 8 dm^3). After freeze-drying, pure 12 was obtained in 98 % yield (0.61 g; DS = 8-9 %; Mw = 105 kDa). ^{1}H NMR (D_2O, 400 MHz): δ 2.00 (overlapped s, H3, H7'), 3.32-4.00 (um, β-CD, HA), 4.47 (um, H1a/H1b),

4.53 (um, H1a/H1b), 4,99 (um, β-CD), 5.01 (um, β-CD), 5.06 (um, β-CD), 5.18 (um, β-CD), 8.24 (s, H4') ppm. The collected data are in agreement with those previously published (Kovacevic et al., 2019).

4.2.18. Propargylamido-HA (13)

The product was prepared according to a slightly modified, previously published procedure (Huerta-Angeles et al., 2011). First, hyalur-onan acid form was prepared as follows. To the sodium hyaluronate (600 kDa; 1.5 g) dissolved in 100 cm^3 of demineralised water, 6 g of DOWEX 50WX4 cation exchange resin was added. After 4 h, the ion exchange procedure was quenched by removing the resin beads by filtration and the filtrate was freeze-dried. 0.5 g (1.32 mmol; Mw = 200 kDa) of obtained acid form of HA was dissolved in 50 cm^3 of dry DMSO at an elevated temperature (60 °C). The solution was then allowed to cool down to room temperature. Next, 0.92 cm^3 (6.6 mmol; 5 eq.) of TEA was added, and the mixture was stirred for 10 min followed by the addition of 0.4 cm^3 (3.0 mmol; 2.3 eq.) of ethyl chloroformate. After stirring the reaction mixture for 1 h, propargylamine (0.1 cm^3; 1.32 mmol) was added and the reaction was allowed to proceed overnight. The reaction mixture was then cooled in an ice-bath, diluted with 50 cm^3 of water and dialysed (cut-off 14 kDa) against 0.1 M NaCl solution (2 x 8 dm^3) and then water (6 x 8 dm^3). After freeze-drying, pure 13 was obtained in 92 % yield (0.46 g; DS = 25 %; Mw = 135 kDa). ^{1}H NMR (D_2O, 400 MHz): δ 2.00 (um, 3H, NHAc), 3.35 (um, HA), 3.51 (um, HA), 3.72 (um, HA), 3.81 (um, HA), 3.91 (um, HA), 3.98 (d, 1H, $^2J_{H,H}$ = 18 Hz), 4.10 (d, 1H, $^2J_{H,H}$ = 18 Hz), 4.53 (um, 2H, HA) ppm. The collected data are in agreement with those previously published (Huerta-Angeles et al., 2011).

4.2.19. β-Cyclodextrin-modified propargylamido-HA (14)

The product was prepared according to a modified, previously published procedure. (Huerta-Angeles et al., 2011) Propargylamido-HA 13 (0.41 g; 1.01 mmol; DS = 25 %; Mw = 135 kDa) was dissolved in 55 cm^3 of 0.1 M phosphate-buffered saline solution (PBS; pH 7.4). Subsequently, solid compound 9 (0.58 g; 0.5 mmol), CuSO4-5H2O (0.05 g; 0.2 mmol) and sodium ascorbate (0.05 g; 0.25 mmol) were added to the solution. The reaction mixture was then stirred vigorously overnight at room temperature. The product was purified by dialysis (cut-off 14 kDa) against 0.01 % EDTA (2 x 8 dm^3) and then water (6 x 8 dm^3). After freeze-drying, pure 14 was obtained in 90 % yield (0.64 g; DS = 25 %; Mw = 26 kDa). ^{1}H NMR (D2O, 400 MHz): δ 2.00 (overlapped s, H3, H7'), 3.35-4.00 (um, β-CD, HA), 4.47 (um, H1a/H1b), 4.53 (um, H1a/H1b), 4.98 (um, β-CD), 5.02 (um, β-CD), 5.17 (um, β-CD), 7.98 (s, H3') ppm.

References

Alizadehgiashi, M., Khuu, N., Khabibullin, A., Henry, A., Tebbe, M., Suzuki, T., & Kumacheva, E. (2018). Nanocolloidal hydrogel for heavy metal scavenging. ACS Nano, 12, 8160-8168. https://doi.org/10.1021/acsnano.8b03202

Barrow, S. J., Kasera, S., Rowland, M. J., Barrio, J., & Scherman, O. A. (2015). Cucurbituril-based molecular recognition. Chemical Review, 115, 12320-12406. https://doi.org/10.1021/acs.chemrev.5b00341

Bermejo-Velasco, D., Azémar, A., Oommen, O., Hilborn, J., & Varghese, O. (2019). Modulating thiol pKa promotes disulfide formation at physiological pH: An elegant strategy to design disulfide cross-linked hyaluronic acid hydrogels. Biomacromolecules, 20, 1412-1420. https://doi.org/10.1021/acs.biomac.8b01830

Bi, B., Ma, M., Lv, S., Zhuo, R., & Jiang, X. (2019). In-situ forming thermosensitive hydroxypropyl chitin-based hydrogel crosslinked by diels-Alder reaction for three dimensional cell culture. Carbohydrate Polymers, 212, 368-377. https://doi.org/ 10.1016/j.carbpol.2019.02.058

Boehnke, N., Cam, C., Bat, E., Segura, T., & Maynard, H. (2015). Imine hydrogels with tunable degradability for tissue engineering. Biomacromolecules, 16, 2101-2108. https://doi.org/10.1021/acs.biomac.5b00519

Burillo, J., Ballinas, L., Burillo, G., Guerrero-Lestarjette, E., Lardizabal-Gutierrez, D., & Silva-Hidalgo, H. (2021). Chitosan hydrogel synthesis to remove arsenic and fluoride ions from groundwater. Journal of Hazardous Materials, 417, Article 126070. https:// doi.org/10.1016/j.jhazmat.2021.126070

Cao, L., Sekutor, M., Zavalij, P., Mlinarié-Majerski, K., Glaser, R., & Isaacs, L. (2014). Cucurbit[7]urilGuest pair with an attomolar dissociation constant. Angewandte Chemie, 126, 1006-1011. https://doi.org/10.1002/ange.201309635

Chen, J., Yang, J., Wang, L., Zhang, X., Heng, B., Wang, D., & Ge, Z. (2021). Modified hyaluronic acid hydrogels with chemical groups that facilitate adhesion to host tissues enhance cartilage regeneration. Bioactive Materials, 6, 1689-1698. https:// doi.org/10.1016/j.bioactmat.2020.11.020

Chen, R., Li, Y., Jin, Y., Sun, Y., Zhao, Z., Xu, Y., Xu, J.-F., Dong, Y., & Liu, D. (2023). Reinforcing supramolecular hyaluronan hydrogels via kinetically interlocking multiple-units strategy. Carbohydrate Polymers, 310, Article 120703. https://doi.org/ 10.1016/j.carbpol.2023.120703

Chen, X., Dong, C., Wei, K., Yao, Y., Feng, Q., Zhang, K., Han, F., Mak, A. F.-T., Li, B., & Bian, L. (2018). Supramolecular hydrogels cross-linked by preassembled host-guest PEG cross-linkers resist excessive, ultrafast, and non-resting cyclic compression. NPG Asia Materials, 10, 788-799. https://doi.org/10.1038/s41427-018-0071-0

Crini, G. (2014). Review: A history of cyclodextrins. Chemical Reviews, 114, 10940-10975. https://doi.org/10.1021/cr500081p

Dai, X., Huo, M., Dong, X., Hu, Y., & Liu, Y. (2022). Noncovalent polymerization-activated ultrastrong near-infrared room-temperature phosphorescence energy transfer assembly in aqueous solution. Advanced Materials, 34, Article 2203534. https://doi.org/10.1002/adma.202203534

Engkagul, V., Sereemaspun, A., & Chirachanchai, S. (2018). One pot preparation of chitosan/hyaluronic acid-based triple network hydrogel via in situ click reaction, metal coordination and polyion complexation in water. Carbohydrate Polymers, 200, 616-623. https://doi.org/10.1016Zj.carbpol.2018.07.090

Facchin, M., Scarso, A., Selva, M., Perosa, A., & Riello, P. (2017). Towards life in hydrocarbons: Aggregation behaviour of “reverse” surfactants in cyclohexane. RSC Advances, 7, 15337-15341. https://doi.org/10.1039/C7RA01027C

Freeman, W., Mock, W., & Shih, N. (1981). Cucurbituril. Journal of the American Chemical Society, 103, 7367-7368. https://doi.org/10.1021/ja00414a070

Gao, F., Bi, Z., Wang, S., Zhao, Z., Dong, Y., & Li, X. (2022). An amphiphilic azobenzene derivative as a crosslinker in the construction of smart supramacromolecular hydrogels. Colloids and Surfaces A: Physicochemical and Engineering Aspects, 647, Article 129088. https://doi.org/10.1016/j.colsurfa.2022.129088

Gao, Y., Peng, J., Zhou, M., Yang, Y., Wang, X., Wang, J., Cao, Y., Wang, W., & Wu, D. (2020). A multi-model, large range and anti-freezing sensor based on a multi-crosslinked poly(vinyl alcohol) hydrogel for human-motion monitoring. Journal of Materials Chemistry B, 8, 11010-11020. https://doi.org/10.1039/D0TB02250K

Ghaderinejad, P., Najmoddin, N., Bagher, Z., Saeed, M., Karimi, S., Simorgh, S., & Pezeshki-Modaress, M. (2021). An injectable anisotropic alginate hydrogel containing oriented fibers for nerve tissue engineering. Chemical Engineering Journal, 420, Article 130465. https://doi.org/10.1016/jxej.2021.130465

Hou, S., Wang, X., Park, S., Jin, X., & Ma, P. (2015). Rapid self-integrating, injectable hydrogel for tissue complex regeneration. Advanced Healthcare Materials, 4, 1491-1495. https://doi.org/10.1002/adhm.201500093

Huang, J., Gu, J., Liu, J., Guo, J., Liu, H., Hou, K., Jiang, X., Yang, X., & Guan, L. (2021). Environment stable ionic organohydrogel as a self-powered integrated system for wearable electronics. Journal of Materials Chemistry A, 9, 16345-16358. https://doi. org/10.1039/D1TA03618A

Huang, S., Hou, L., Li, T., Jiao, Y., & Wu, P. (2022a). Antifreezing hydrogel electrolyte with ternary hydrogen bonding for high-performance zinc-ion batteries. Advanced Materials, 34, 2110140. https://doi.org/10.1002/adma.202110140

Huang, Z., Chen, X., O'Neill, S., Wu, G., Whitaker, D., Li, J., McCune, J., & Scherman, O. (2022b). Highly compressible glass-like supramolecular polymer networks. Nature Materials, 21, 103-109. https://doi.org/10.1038/s41563-021-01124-x Huang, Z., Chen, X., Wu, G., Metrangolo, P., Whitaker, D., McCune, J., & Scherman, O. (2020) . Host-enhanced phenyl-perfluorophenyl Polar—n interactions. Journal of the American Chemical Society, 142, 7356-7361. https://doi.org/10.1021/jacs.0c02275

Huerta-Angeles, G., Nemcová, M., Príkopova, E., Smejkalova, D., Pravda, M., Kucera, L., & Velebný, V. (2012). Reductive alkylation of hyaluronic acid for the synthesis of biocompatible hydrogels by click chemistry. Carbohydrate Polymers, 90, 1704-1711. https://doi.org/10.1016/j.carbpol.2012.07.054

Huerta-Angeles, G., Smejkalovaá, D., Chláadkovaá, D., Ehlovaá, T., Buffa, R., & Velebný, V. (2011). Synthesis of highly substituted amide hyaluronan derivatives with tailored degree of substitution and their crosslinking via click chemistry. Carbohydrate Polymers, 84, 1293-1300. https://doi.org/10.1016/jxarbpol.2011.01.021

Hu, C., Long, L., Cao, J., Zhang, S., & Wang, Y. (2021a). Dual-crosslinked mussel-inspired smart hydrogels with enhanced antibacterial and angiogenic properties for chronic infected diabetic wound treatment via pH-responsive quick cargo release. Chemical Engineering Journal, 411, Article 128564. https://doi.org/10.1016/). cej.2021.128564

Hu, Y., Zhang, M., Qin, C., Qian, X., Zhang, L., Zhou, J., & Lu, A. (2021b). Transparent, conductive cellulose hydrogel for flexible sensor and triboelectric nanogenerator at subzero temperature. Carbohydrate Polymers, 265, Article 118078. https://doi.org/ 10.1016/j.carbpol.2021.118078

Jarrell, D., Vanderslice, E., Lennon, M., Lyons, A., VeDepo, M., Jacot, J., & Jabbari, E. (2021) . Increasing salinity of fibrinogen solvent generates stable fibrin hydrogels for cell delivery or tissue engineering. PLOS ONE, 16, 1-16. https://doi.org/10.1371/ journal.pone.0239242

Jiang, Y., Pan, X., Chang, J., Niu, W., Hou, W., Kuai, H., Zhao, Z., Liu, J., Wang, M., & Tan, W. (2018). Supramolecularly engineered circular bivalent aptamer for enhanced functional protein delivery. Journal of the American Chemical Society, 140, 6780-6784. https://doi.org/10.1021/jacs.8b03442

Jin, R., Xu, J., Duan, L., & Gao, G. (2021). Chitosan-driven skin-attachable hydrogel sensors toward human motion and physiological signal monitoring. Carbohydrate Polymers, 268, Article 118240. https://doi.org/10.1016/jxarbpol.2021.118240

Ji, S., Abaci, A., Morrison, T., Gramlich, W., & Guvendiren, M. (2020). Novel bioinks from UV-responsive norbornene-functionalized carboxymethyl cellulose macromers. Bioprinting, 18, Article e00083. https://doi.org/10.1016/j.bprint.2020.e00083

Johnson, C. S. (1999). Diffusion ordered nuclear magnetic resonance spectroscopy: Principles and applications. Progress in Nuclear Magnetic Resonance Spectroscopy, 34, 203-256. https://doi.org/10.1016/S0079-6565(99)00003-5

Kang, W., Bi, B., Zhuo, R., & Jiang, X. (2017). Photocrosslinked methacrylated carboxymethyl chitin hydrogels with tunable degradation and mechanical behavior. Carbohydrate Polymers, 160, 18-25. https://doi.org/10.1016/jxarbpol.2016.12.032

Kim, J., Jung, I., Kim, S., Lee, E., Kang, J., Sakamoto, S., Yamaguchi, K., & Kim, K. (2000). New cucurbituril homologues: Syntheses, isolation, characterization, and X-ray crystal structures of Cucurbit[n]uril (n = 5, 7, and 8). Journal of the American Chemical Society, 122, 540-541. https://doi.org/10.1021/ja993376p

Kolewe, K., Zhu, J., Mako, N., Nonnenmann, S., & Schiffman, J. (2018). Bacterial adhesion is affected by the thickness and stiffness of Poly(ethylene glycol) hydrogels. ACS Applied Materials & Interfaces, 10, 2275-2281. https://doi.org/10.1021/ acsami.7b12145

Korosec, E., Poljsak, D., & Urleb, U. (1992). Synthesis of N-acylamino-ethoxyacetic acid derivatives. Archiv der Pharmazie, 325, 251-252. https://doi.org/10.1002/ ardp.19923250412

Kovaceviác, J., Pruckováa, Z., Pospísil, T., Kaspaárkovaá, V., Rouchal, M., & Vícha, R. (2019). A new hyaluronan modified with p-cyclodextrin on hydroxymethyl groups forms a dynamic supramolecular network. Molecules, 24, 3849. https://doi.org/10.3390/ molecules24213849

Kwon, T., Jeong, Y. K., Deniz, E., AlQaradawi, S. Y., Choi, J. W., & Coskun, A. (2015). Dynamic cross-linking of polymeric binders based on host-guest interactions for silicon anodes in lithium ion batteries. ACS Nano, 9, 11317-11324. https://doi.org/ 10.1021/acsnano.5b05030

Lei, Y., Wang, X., Liao, J., Shen, J., Li, Y., Cai, Z., Hu, N., Luo, X., Cui, W., & Huang, W. (2022) . Shear-responsive boundary-lubricated hydrogels attenuate osteoarthritis. Bioactive Materials, 16, 472-484. https://doi.org/10.1016/j.bioactmat.2022.02.016

Li, D., Yang, Z., Luo, Y., Zhao, X., Tian, M., & Kang, P. (2022a). Delivery of MiR335-5p-pendant tetrahedron DNA nanostructures using an injectable heparin lithium hydrogel for challenging bone defects in steroid-associated osteonecrosis. Advanced Healthcare Materials, 11, 2101412. https://doi.org/10.1002/adhm.202101412

Li, H., Zhou, X., Luo, L., Ding, Q., & Tang, S. (2022b). Bio-orthogonally crosslinked catechol-chitosan hydrogel for effective hemostasis and wound healing.Carbohydrate Polymers, 281, Article 119039. https://doi.org/10.1016/j. carbpol.2021.119039

Li, S., Zhao, X., Wang, Q., Yu, F., Li, W., Bai, Y., Shen, X., Du, X., He, D., & Yuan, J. (2022c). Mechanoresponsive drug loading system with tunable host-guest interactions for ocular disease treatment. ACS Biomaterials Science & Engineering, 8, 4850-4862. https://doi.org/10.1021/acsbiomaterials.2c00931

Li, S., Dong, Q., Peng, X., Chen, Y., Yang, H., Xu, W., Zhao, Y., Xiao, P., & Zhou, Y. (2022d). Self-healing hyaluronic acid nanocomposite hydrogels with platelet-rich plasma impregnated for skin regeneration. ACS Nano, 16, 11346-11359. https://doi. org/10.1021/acsnano.2c05069

Liu, H., Ni, Y., Hu, J., Jin, Y., Gu, P., Qiu, H., & Chen, K. (2022a). Self-healing and antibacterial essential oil-loaded mesoporous Silica/Polyacrylate hybrid hydrogel for high-performance wearable body-strain sensing. ACS Applied Materials & Interfaces, 14, 21509-21520. https://doi.org/10.1021/acsami.2c03406

Liu, Y., Wang, J., Chen, H., & Cheng, D. (2022b). Environmentally friendly hydrogel: A review of classification, preparation and application in agriculture. Science of the Total Environment, 846, Article 157303. https://doi.org/10.1016/j. scitotenv.2022.157303

Lu, Q., Han, Y., Ma, Y., & Lv, S. (2022). Design of silk fibroin-based supramolecular hydrogels through host-guest interactions: Influence of the crosslinking type. Colloids and Surfaces A: Physicochemical and Engineering Aspects, 652, Article 129898. https:// doi.org/10.1016/j.colsurfa.2022.129898

Mealy, J., Rodell, C., & Burdick, J. (2015). Sustained small molecule delivery from injectable hyaluronic acid hydrogels through host-guest mediated retention. Journal of Materials Chemistry B, 3, 8010-8019. https://doi.org/10.1039/C5TB00981B

Mo, F., Huang, Y., Li, Q., Wang, Z., Jiang, R., Gai, W., & Zhi, C. (2021). A highly stable and durable capacitive strain sensor based on dynamically super-tough hydro/ organo-gels. Advanced Functional Materials, 31, 2010830. https://doi.org/10.1002/ adfm.202010830

Mol, E., Lei, Z., Roefs, M., Bakker, M., Goumans, M., Doevendans, P., Dankers, P., Vader, P., & Sluijter, J. (2019). Injectable supramolecular ureidopyrimidinone hydrogels provide sustained release of extracellular vesicle therapeutics. Advanced Healthcare Materials, 8, 1900847. https://doi.org/10.1002/adhm.201900847

Mueller, E., Poulin, I., Bodnaryk, W., & Hoare, T. (2022). Click chemistry hydrogels for extrusion bioprinting: Progress, challenges, and opportunities. Biomacromolecules, 23, 619-640. https://doi.org/10.1021/acs.biomac.1c01105

Muir, V., & Burdick, J. (2021). Chemically modified biopolymers for the formation of biomedical hydrogels. Chemical Reviews, 121, 10908-10949. https://doi.org/ 10.1021/acs.chemrev.0c00923

Neisi, E., Tehrani, A., & Shamlouei, H. (2023). Fully bio-based supramolecular gel based on cellulose nanowhisker gallate by cyclodextrin host-guest chemistry. Carbohydrate Polymers, 299, Article 120222. https://doi.org/10.1016/jxarbpol.2022.120222

Nielsen, T., Wintgens, V., Amiel, C., Wimmer, R., & Larsen, K. (2010). Facile synthesis of P-cyclodextrin-dextran polymers by “Click” chemistry. Biomacromolecules, 11, 1710-1715. https://doi.org/10.1021/bm9013233

Nilasaroya, A., Kop, A., & Morrison, D. (2021). Heparin-functionalized hydrogels as growth factor-signaling substrates. Journal of Biomedical Materials Research Part A, 109, 374-384. https://doi.org/10.1002/jbm.a.37030

Ooi, H. W., Kocken, J. M. M., Morgan, F. L. C., Malheiro, A., Zoetebier, B., Karperien, M., Wieringa, P. A., Dijkstra, P. J., Moroni, L., & Baker, M. B. (2020). Multivalency enables dynamic supramolecular host— guest hydrogel formation. Biomacromolecules, 21, 2208-2217. https://doi.org/10.1021/acs.biomac.0c00148

Otremba, T., & Ravoo, B. (2017). Dynamic multivalent interaction of phenylboronic acid functionalized dendrimers with vesicles. Tetrahedron, 73, 4972-4978. https://doi. org/10.1016/j.tet.2017.04.043

Petter, R., Salek, J., Sikorski, C., Kumaravel, G., & Lin, F. (1990). Cooperative binding by aggregated mono-6-(alkylamino)-P-cyclodextrins. Journal of the American Chemical Society, 112, 3860-3868. https://doi.org/10.1021/ja00166a021

Phua, S., Yang, G., Lim, W., Verma, A., Chen, H., Thanabalu, T., & Zhao, Y. (2019). Catalase-integrated hyaluronic acid as nanocarriers for enhanced photodynamic therapy in solid tumor. ACS Nano, 13, 4742-4751. https://doi.org/10.1021/ acsnano.9b01087

Rosales, A., Rodell, C., Chen, M., Morrow, M., Anseth, K., & Burdick, J. (2018). Reversible control of network properties in azobenzene-containing hyaluronic acid-based hydrogels. Bioconjugate Chemistry, 29, 905-913. https://doi.org/10.1021/acs. bioconjchem.7b00802

Rowland, M., Parkins, C., McAbee, J., Kolb, A., Hein, R., Loh, X., Watts, C., & Scherman, O. (2018). An adherent tissue-inspired hydrogel delivery vehicle utilised in primary human glioma models. Biomaterals, 179, 199-208. https://doi.org/ 10.1016/j.biomaterials.2018.05.054

Samanta, A., Tesch, M., Keller, U., Klingauf, J., Studer, A., & Ravoo, B. (2015). Fabrication of hydrophilic polymer nanocontainers by use of supramolecular templates. Journal of the American Chemical Society, 137, 1967-1971. https://doi. org/10.1021/ja511963g

Saunders, L., & Ma, P. (2019). Self-healing supramolecular hydrogels for tissue engineering applications. Macromolecular Bioscience, 19, 1800313. https://doi.org/ 10.1002/mabi.201800313

Shin, J., Yeo, Y., Jeong, J., Park, S., & Park, W. (2020). Dual-crosslinked methylcellulose hydrogels for 3D bioprinting applications. Carbohydrate Polymers, 238, Article 116192. https://doi.org/10.1016/jxarbpol.2020.116192

Shin, M., Song, K., Burrell, J., Cullen, D., & Burdick, J. (2019). Injectable and conductive granular hydrogels for 3D printing and electroactive tissue support. Advanced Science, 6, 1901229. https://doi.org/10.1002/advs.201901229

Shu, L., Zhang, X., Wang, Z., & Yao, J. (2022). Structure reorganization of cellulose hydrogel by green solvent exchange for potential plastic replacement. Carbohydrate Polymers, 275, Article 118695. https://doi.org/10.1016/jxarbpol.2021.118695

Schneider, H., Hacket, F., Rudiger, V., & Ikeda, H. (1998). NMR studies of cyclodextrins and cyclodextrin complexes. Chemical Reviews, 98, 1755-1786. https://doi.org/ 10.1021/cr970019t

Sinha, S., Ayushman, M., Tong, X., & Yang, F. (2023). Dynamically crosslinked Poly (ethylene-glycol) hydrogels reveal a critical role of viscoelasticity in modulating glioblastoma fates and drug responses in 3D. Advanced Healthcare Materals, 12, 2202147. https://doi.org/10.1002/adhm.202202147

Sudhadevi, T., Vijayakumar, H., Hariharan, E., Sandhyamani, S., & Krishnan, L. (2021). Optimizing fibrin hydrogel toward effective neural progenitor cell delivery in spinal cord injury. Biomedical Materials, 17, Article 014102. https://doi.org/10.1088/1748-605X/ac3680

Šedová, P., Buffa, R., Kettou, S., Huerta-Angeles, G., Hermannová, M., Leierová, V., Smejkalová, D., Moravcová, M., & Velebný, V. (2013). Preparation of hyaluronan polyaldehyde—A precursor of biopolymer conjugates. Carbohydrate Research, 371, 8-15. https://doi.org/10.1016/jcarres.2013.01.025

Tang, S., Yang, J., Lin, L., Peng, K., Chen, Y., Jin, S., & Yao, W. (2020). Construction of physically crosslinked chitosan/sodium alginate/calcium ion double-network hydrogel and its application to heavy metal ions removal. Chemical Engineering Journal, 393, Article 124728. https://doi.org/10.1016Zj.cej.2020.124728

Tomeček, J., Cablová, A., Hromadková, A., Novotný, J., Marek, R., Durník, I., Kulhánek, P., Prucková, Z., Rouchal, M., Dastychova, L., & Vícha, R. (2021). Modes of micromolar host-guest binding of p-cyclodextrin complexes revealed by NMR spectroscopy in salt water. The Journal of Organic Chemistry, 86, 4483-4496. https:// doi.org/10.1021/acs.joc.0c02917

Trotta, F., Loftsson, T., Gaud, R., Trivedi, R., & Shende, P. (2022). Integration of cyclodextrins and associated toxicities: A roadmap for high quality biomedical applications. Carbohydrate Polymers, 295, Article 119880. https://doi.org/10.1016/ j.carbpol.2022.119880

Wang, L., Highley, C., Yeh, Y., Galarraga, J., Uman, S., & Burdick, J. (2018). Threedimensional extrusion bioprinting of single- and double-network hydrogels containing dynamic covalent crosslinks. Journal of Biomedical Materials Research Part A, 106, 865-875. https://doi.org/10.1002/jbm.a.36323

Wei, K., Zhu, M., Sun, Y., Xu, J., Feng, Q., Lin, S., Wu, T., Xu, J., Tian, F., Xia, J., Li, G., & Bian, L. (2016). Robust biopolymeric supramolecular "host— guest macromer" hydrogels reinforced by in situ formed multivalent nanoclusters for cartilage regeneration. Macromolecules, 49, 866-875. https://doi.org/10.1021/acs. macromol.5b02527

Wu, S., Hua, M., Alsaid, Y., Du, Y., Ma, Y., Zhao, Y., Lo, C., Wang, C., Wu, D., Yao, B., Strzalka, J., Zhou, H., Zhu, X., & He, X. (2021). Poly(vinyl alcohol) hydrogels with broad-range tunable mechanical properties via the hofmeister effect. Advanced Materials, 33, 2007829. https://doi.org/10.1002/adma.202007829

Wu, Y., Shah, D., Liu, C., Yu, Z., Liu, J., Ren, X., Rowland, M., Abell, C., Ramage, M., & Scherman, O. (2017). Bioinspired supramolecular fibers drawn from a multiphase self-assembled hydrogel. Proceedings of the National Academy of Sciences, 114, 8163-8168. https://doi.org/10.1073/pnas.1705380114

Xia, D., Wang, P., Ji, X., Khashab, N., Sessler, J., & Huang, F. (2020). Functional supramolecular polymeric networks: The marriage of covalent polymers and macrocycle-based host-guest interactions. Chemical Reviews, 120, 6070-6123. https://doi.org/10.1021/acs.chemrev.9b00839

Xue, X., Liang, K., Huang, W., Yang, H., Jiang, L., Jiang, Q., Jiang, T., Lin, B., Chen, Y., Jiang, B., & Komarneni, S. (2022). Molecular engineering of injectable, fast selfrepairing hydrogels with tunable gelation time: Characterization by diffusing wave spectroscopy. Macromolecules, 55, 6474-6486. https://doi.org/10.1021/acs. macromol.2c00899

Xu, C., Zhan, W., Tang, X., Mo, F., Fu, L., & Lin, B. (2018). Self-healing chitosan/vanillin hydrogels based on schiff-base bond/hydrogen bond hybrid linkages. Polymer Testing, 66, 155-163. https://doi.org/10.1016Zj.polymertesting.2018.01.016

Xu, Y., Cui, M., Patsis, P., Gunther, M., Yang, X., Eckert, K., & Zhang, Y. (2019). Reversibly assembled electroconductive hydrogel via a host-guest interaction for 3D cell culture. ACS Applied Materials & Interfaces, 11, 7715-7724. https://doi.org/ 10.1021/acsami.8b19482

Yang, J., Chen, Y., Zhao, L., Zhang, J., & Luo, H. (2022). Constructions and properties of physically cross-linked hydrogels based on natural polymers. Polymer Reviews, 2022, 1-39. https://doi.org/10.1080/15583724.2022.2137525

Yang, P., Feng, C., Liu, Y., Cheng, T., Yang, X., Liu, H., Liu, K., & Fan, H. (2020). Thermal self-protection of zinc-ion batteries enabled by smart hygroscopic hydrogel electrolytes. Advanced Energy Materials, 10, 2002898. https://doi.org/10.1002/ aenm.202002898

Yao, Y., Zaw, A., Anderson, D., Hinds, M., & Yim, E. (2020). Fucoidan functionalization on poly(vinyl alcohol) hydrogels for improved endothelialization and hemocompatibility. Biomaterials, 249, Article 120011. https://doi.org/10.1016/j. biomaterials.2020.120011

Yavvari, P., Pal, S., Kumar, S., Kar, A., Awasthi, A., Naaz, A., Srivastava, A., & Bajaj, A. (2017). Injectable, self-healing chimeric catechol-Fe(III) hydrogel for localized combination cancer therapy. ACS Biomaterials Science & Engineering, 3, 3404-3413. https://doi.org/10.1021/acsbiomaterials.7b00741

Yu, B., Zhan, A., Liu, Q., Ye, H., Huang, X., Shu, Y., Yang, Y., & Liu, H. (2020). A designed supramolecular cross-linking hydrogel for the direct, convenient, and efficient administration of hydrophobic drugs. International Journal of Pharmaceutics, 578, Article 119075. https://doi.org/10.1016/jijpharm.2020.119075

Yuan, Y., Zhang, H., & Qu, J. (2021). Pyridine-dicarbohydrazone-based polyacrylate hydrogels with strong mechanical property, tunable/force-induced fluorescence, and thermal/pH stimuli responsiveness. ACS Applied Polymer Materials, 3, 4512-4522. https://doi.org/10.1021/acsapm.1c00541

Zatloukal, F., Achbergerovaá, E., Gergela, D., Rouchal, M., Dastychováa, L., Pruckovaá, Z., & Vícha, R. (2021). Supramolecular properties of amphiphilic adamantylated azo dyes. Dyes and Pigments, 192, Article 109420. https://doi.org/10.1016/j. dyepig.2021.109420

Zhang, B., He, J., Shi, M., Liang, Y., & Guo, B. (2020). Injectable self-healing supramolecular hydrogels with conductivity and photo-thermal antibacterial activity to enhance complete skin regeneration. Chemical Engineering Journal, 400, Article 125994. https://doi.org/10.1016/jcej.2020.125994

Zhang, D., Jian, J., Xie, Y., Gao, S., Ling, Z., Lai, C., Wang, J., Wang, C., Chu, F., & Dumont, M. (2022a). Mimicking skin cellulose hydrogels for sensor applications. Chemical Engineering Journal, 427, Article 130921. https://doi.org/10.1016/j. cej.2021.130921

Zhang, H., Xia, H., & Zhao, Y. (2012). Poly(vinyl alcohol) hydrogel can autonomously self-heal. ACS Macro Letters, 1, 1233-1236. https://doi.org/10.1021/mz300451r

Zhang, C., Wang, S., Zhang, P., Xu, S., Song, Z., Chen, J., Chen, S., & Zeng, R. (2021). Cellular and mitochondrial dual-targeted nanoprobe with near-infrared emission for activatable tumor imaging and photodynamic therapy. Sensors and Actuators B: Chemical, 346, Article 130451. https://doi.org/10.1016/j.snb.2021.130451

Zhang, J., Hurren, C., Lu, Z., & Wang, D. (2022b). pH-sensitive alginate hydrogel for synergistic anti-infection. International Journal of Biological Macromolecules, 222, 1723-1733. https://doi.org/10.1016/jijbiomac.2022.09.234

Zhang, Y., Zheng, Y., Shu, F., Zhou, R., Bao, B., Xiao, S., Li, K., Lin, Q., Zhu, L., & Xia, Z. (2022c). In situ-formed adhesive hyaluronic acid hydrogel with prolonged amnion-derived conditioned medium release for diabetic wound repair. Carbohydrate Polymers, 276, Article 118752. https://doi.org/10.1016/jcarbpol.2021.118752

Zhao, H., & Heindel, N. (1991). Determination of degree of substitution of formyl groups in polyaldehyde dextran by the hydroxylamine hydrochloride method. Pharmaceutical Research, 08, 400-402. https://doi.org/10.1023/A:1015866104055

Zhou, T., Xiong, H., Wang, S., Zhang, H., Zheng, W., Gou, Z., Fan, C., & Gao, C. (2022a). An injectable hydrogel dotted with dexamethasone acetate-encapsulated reactive oxygen species-scavenging micelles for combinatorial therapy of osteoarthritis. Materials Today Nano, 17, Article 100164. https://doi.org/10.1016/j. mtnano.2021.100164

Zhou, T., Ran, J., Xu, P., Shen, L., He, Y., Ye, J., Wu, L., & Gao, C. (2022b). A hyaluronic acid/platelet-rich plasma hydrogel containing MnO2 nanozymes efficiently alleviates osteoarthritis in vivo. Carbohydrate Polymers, 292, Article 119667. https:// doi.org/10.1016/j.carbpol.2022.119667

Zhu, Y., Yang, Z., Pan, Z., Hao, Y., Wang, C., Dong, Z., Li, Q., Han, Y., Tian, L., Feng, L., & Liu, Z. (2022). Metallo-alginate hydrogel can potentiate microwave tumor ablation for synergistic cancer treatment. Science Advances, 8, 1-14. https://doi.org/10.1126/ sciadv.abo5285

Ziemkiewicz, N., Hilliard, G., Dunn, A., Madsen, J., Haas, G., Au, J., Genovese, P., Chauvin, H., West, C., Paoli, A., & Garg, K. (2022). Laminin-111-enriched fibrin hydrogels enhance functional muscle regeneration following trauma. Tissue Engineering Part A, 28, 297-311. https://doi.org/10.1089/ten.tea.2021.0096